THE EFFECT OF SALT ON THE CHEMICAL POTENTIAL OF NEUTRAL MACROMOLECULES DETERMINED BY TERNARY DIFFUSION COEFFICIENTS

by

CONG TAN

Bachelor of Science, 2004
University of Science and Technology of China
Hefei, P.R.China

Submitted to the Graduate Faculty of the
College of Science and Engineering
Texas Christian University
In partial fulfillment of the requirements
for the degree of

Master of Science

December, 2007

Acknowledgments

I would like to acknowledge Dr. Onofrio Annunziata for his invaluable guidance and constant patience during the process of this project.

I would also thank Dr. Albright, who gave me a lot of help and guidance in understanding and operating of his precious Gosting diffusiometer.

I wish to thank my colleagues: Huixiang Zhang, Dongmei Fan and Jian Cui for their generous help and discussion which inspire me often.

I wish to acknowledge Texas Christian University for providing me such a precious opportunity to study here. I also wish to acknowledge TCU research and creative activity funds for financial support.

Finally, I would like to thank my parents for their constant support and love.

TABLE OF CONTENTS

List of Figures

Chapter 2

Chapter 4

Chapter 5

List of Tables

Chapter 1

Background

Introduction

Macromolecules have been extensively studied because of their great importance in a wide range of disciplines. For example, they are the building blocks for many synthetic materials. [1–3] In living organisms, most biological functions are performed by macromolecules. Solutions containing macromolecules are also very important. For example, they are used for the preparation of macromolecular materials and in the investigation of individual macromolecules for physicochemical and biochemical studies. [4,5] Among all employed solvents water, which is also directly relevant to biochemical studies, is normally used for hydrophilic macromolecules. One source of complexity in macromolecular solutions is the presence of other solutes (additives) besides the solvent. [6–15] Thus macromolecular solutions are usually multicomponent in nature.

One important aspect of macromolecular solutions is their thermodynamic behavior, which is described by the chemical potentials of the solution components. The chemical potential of macromolecules in aqueous solution is perturbed by the presence of additives such as salts and small organic molecules. [10–15] The primary thermodynamic effects of these additives on macromolecules are believed to be preferential solvation, binding, and Donnan equilibrium (for charged macromolecules). Understanding how the chemical potential of a macromolecule is affected by the concentration and nature of additives is

important for characterizing free-energy changes of individual macromolecules. These changes may be related to conformational changes of the macromolecule in solution such as coil-to-globule transitions or to changes in solvation of the macromolecules. [10,15] Understanding the dependence of the macromolecule chemical potential on additive concentration is also a necessary step for describing the phase behavior of macromolecular solutions. [18–20] Indeed the addition of additives to the macromolecular solution may induce phase transitions such as liquid-liquid phase separation and crystallization. [19–24] Liquid-liquid phase separation is important for two-liquid partitioning, for extraction/purification applications, and for the preparation of microspheres and nanoparticles for applications in the field of drug delivery and catalysis. Crystallization finds applications in the preparation of bulk macromolecular materials and in the investigation of the structure of macromolecules using X-ray diffraction.[25-27]

Macromolecule-additive preferential-interaction coefficients, which are thermodynamically linked to the dependence of the macromolecule chemical potential on additive concentration, are the primary thermodynamic parameters used to characterize macromolecule-additive interaction.[29-33] These coefficients have been interpreted in terms of models based on the existence of two domains. The first domain is represented by the water-additive layer surrounding individual macromolecules. This local domain is in chemical equilibrium with a bulk domain, representing the water-additive remaining solution. Since macromolecules interact with the additive and water molecules in their

vicinity, the concentration of additive in the local domain is different from that of the unperturbed bulk domain. If the additive concentration in the local domain is lower than that of the bulk domain, preferential hydration of the macromolecules occurs. In this case, the preferential-interaction coefficient is negative. On the other hand, a positive value of this coefficient is obtained if the macromolecules preferentially interact with the additive.

Several thermodynamic studies on macromolecule-additive aqueous solutions have been reported. Equilibrium dialysis and vapor pressure osmosis have been used to determine preferential-interaction coefficients. The experimental and theoretical work of Timasheff [31, 34-36] and Record [33, 37-39] has been of fundamental importance for understanding the thermodynamic concept of preferential interaction using the two-domain model discussed above. Recently, a novel method based on multicomponent diffusion has been introduced for the determination of preferential-interaction coefficients. This method has been applied to lysozyme (a model protein) in the presence of several salts (i.e. KCl, NaCl, NH_4Cl, $MgCl_2$ and $MgCl_2$ at 25 ºC. The precision of these thermodynamic data, which is found to be higher than that obtained by other techniques, has allowed us to 1) reproduce salt ranking of protein precipitant effectiveness, 2) accurately describe not only the nature and magnitude of the thermodynamic interaction but also its dependence on salt concentration.

Another important aspect of macromolecule-additive aqueous solutions is their dynamic behavior in the presence of concentration gradients. This is described by multicomponent diffusion coefficients.[2, 40] Concentration gradients occur in a large number of in vivo, laboratory, medical, and manufacturing applications. Examples include centrifugation, dialysis, vaporization and crystallization.[1,2] Effective modeling, prediction, and design of these processes require accurate descriptions of macromolecule transport. Recently, applications in which convection is eliminated, and diffusion which becomes the dominant transport mechanism, are increasing important.[40, 41] This is because diffusion, compared to convection, is a more controllable and reproducible process. Convection-free conditions can be obtained by employing gels, capillaries or microgravity. Furthermore, diffusive mass-transfer plays also a crucial role in the emerging microfluidic technologies.[41-45] One example of diffusion-based applications is the counter-diffusion method. Here, the effect of spatial and temporal changes of a chemical environment on a target molecule is investigated by interfacing a solution containing the target molecule with one containing an additive. For macromolecule-crystallization applications, a counter-diffusion experiment consists of interfacing a macromolecular solution with a precipitant solution. Due to the initial large gradients of both macromolecule and precipitant, multicomponent diffusion data become critical for an accurate description of a counter-diffusion experiment and for optimizing the design of initial conditions and instrument setup.

The dependence of the macromolecule chemical potential on salt concentration is also central for understanding diffusive mass transport in macromolecule-additive-water systems.[18-20] This is because diffusive fluxes are driven by chemical-potential gradients in the system. One consequence of this fundamental link between diffusion and thermodynamics is that a diffusive flux of one component can be generated even if its own concentration is uniform throughout the system, provided that its chemical potential is not uniform. This chemical-potential gradient can be generated by the presence of a concentration gradient of another component. In the case of a ternary macromolecule-additive-water system, the macromolecule(1)-additive(2) coupled diffusion can be described by a matrix of four diffusion coefficients defined by Fick's first law:

$$-J_1 = D_{11}\nabla C_1 + D_{12}\nabla C_2 \qquad (1a)$$

$$-J_2 = D_{21}\nabla C_1 + D_{22}\nabla C_2 \qquad (1b)$$

Here, C_1 and C_2 are molar concentrations respectively of protein and salt, J_1 and J_2 are the corresponding fluxes and the four D_{ij}'s (with $i, j = 1, 2$) are the diffusion coefficients. Main diffusion coefficients, D_{11} and D_{22}, describe the flux of a solute due to its own concentration gradient, while cross-diffusion coefficients, D_{12} and D_{21}, describe the flux of a solute due to the concentration gradient of the other solute.

Knowledge of coupled diffusion is important for accurate modeling of mass-transfer processes, especially in the case of large gradients of two solutes. For example, in microfluidic technologies [42] counter-diffusion mixing of two fluids plays a crucial role for the successful mixing of two or more fluids. Furthermore, since molecules diffuse across the boundary layer with different rates, counter-diffusion mixing can be used to selectively transfer solutes from the donating fluid to the receiving fluid. This is the basis of diffusion-based separation and detection technologies.[32] Coupled diffusion could be used for the design of novel applications. Specifically, the concentration gradient of a component 2 can be used as a tool for controlling the diffusion rate of component 1, because $-J_1 = D_{11}\nabla C_1 + D_{12}\nabla C_2$. We believe that the concept of coupled diffusion can be employed in controlled release technologies relevant to drug delivery and microfluidic devices. For example, in the case of drug delivery, the diffusion rate of a drug from a delivery porous device (e.g. gels) could be controlled by the concentration gradient of an inert chemical agent embedded in the device. [28]

Here we report multicomponent-diffusion measurements and preferential-interactions coefficients on the poly(ethylene glycol)-KCl-water ternary system at 25ºC using precision Rayleigh interferometry. This investigation has been motivated by the following three reasons. First, poly(ethylene glycol) (PEG) is a hydrophilic nonionic polymer used in many biochemical, pharmaceutical and industrial applications. [1, 3, 9, 47] Due to its nontoxic character, this chemical can be found in cosmetics, food, and pharmaceutical

products. The mild action of PEG on the biological activity of cell components explains the success of this polymer in biotechnological applications. PEG is commonly used for liquid–liquid partitioning and precipitation of biomacromolecules. In protein crystallography, PEG is considered the most successful precipitating agent for the production of protein crystals, the crucial step for the determination of the molecular structure of a protein.[3, 9] PEG has also been used for the preparation of biomaterial for drug delivery. All these applications make PEG by far the most widely used polymer in aqueous solutions of biological molecules. PEG aqueous systems often include salts. For example, salts can be used to induce liquid-liquid phase separation of PEG aqueous solutions, relevant to liquid-liquid partitioning. Moreover salt and PEG are used together to facilitate protein precipitation. Knowledge of multicomponent diffusion coefficients and thermodynamic parameters on PEG-salt aqueous mixtures is generally important for the PEG applications.[48-49] However, to our knowledge, measurements of preferential-interaction coefficients for these systems have not been reported. Second, preferential-interaction coefficients have been usually determined for protein systems. So a comparison between PEG-salt and protein-salt interactions will be valuable for understanding differences in preferential hydration between PEG and proteins. For this reason, we will compare our results with those previously obtained at this laboritaray on the lysozyme-KCl-water ternary system.[13,49-52] Third, the determination of preferential-interaction coefficients based on multicomponent diffusion assumes the validity of the three postulates of non-equilibrium thermodynamics (see chap 3). Thus an

experimental comparison between our diffusion-based method and postulate-free equilibrium techniques is a very important contribution to both equilibrium and non-equilibrium thermodynamics. For this reason, we have also performed measurements of preferential-interaction coefficients using the isopiestic method and compared these values with those extracted from diffusion measurements. The isopiestic method is a very accurate equilibrium technique normally used for the determination of activity-coefficient data of salt-water solutions. However, this technique is very time consuming compared to the diffusion method, and generally not be suitable for the study of protein solutions.

Poly(ethylene glycol)

PEG is a nonionic polymer with molecular formula:

$$\mathrm{HO}-\left(\mathrm{CH_2CH_2O}\right)_n-\mathrm{H}$$

where *n* is the number of repeating units. For our experiments, we will use PEG with mass average molecular weight 20,000 g mol^{-1}. This corresponds to *n* = 450. It is important to remember that polymers are polydisperse macromolecules. However, PEG polydispersity is rather small compared to many other polymers. Since PEG is prepared by cationic polymerization, its molecular-weight distribution follows the narrow Poisson distribution function.[53,54] Hence, for our PEG, the polydispersity index is $M_w / M_n = 1.04$, where M_w and M_n are the mass-average and number-average molecular weights respectively.

In dilute aqueous solutions, PEG approximately behaves like a random coil at room temperature (dilute regime). As the temperature increases, PEG tends to behave like a compact globule due to PEG-water repulsive interactions. As PEG concentration increases, weak nonbonding PEG-PEG interactions are observed (semidilute regime). At high PEG concentrations, it is believed that a network of PEG molecules mediated by water bridges exists (concentrated regime). The crossover between the dilute and semidilute regime occurs when PEG-PEG contacts occur. For PEG with molecular weight 20,000 g mol^{-1}, the crossover concentration is C^{*} = 1.7 mM. Our experiments have been performed at PEG concentration equal to 25 mM well into the semidilute regime.[55,56]

Chapter 2

Thermodynamics of macromolecule-additive-solvent mixtures

Introduction

Here I review some important thermodynamic aspects of macromolecule-additive-solvent ternary mixtures. Specifically, I will introduce the preferential-interaction coefficient and relate it to the solute chemical potentials. I will use the subscript "1" to identify the macromolecular solute and the subscript "2" to identify the additive, normally a solute with low molecular weight.

Macromolecule(1)-additive(2) thermodynamic interactions are conveniently described by the preferential-interaction coefficient Γ_{12} defined by:

$$\Gamma_{12} = \lim_{m_1 \to 0} \left(\frac{\partial m_2}{\partial m_1} \right)_{T,p,\mu_2} = -\lim_{m_1 \to 0} \frac{\mu_{12}^{(m)}}{\mu_{22}^{(m)}}, \qquad (1)$$

where $\mu_{12}^{(m)} \equiv \left(\partial \mu_1 / \partial m_2\right)_{T,p,m_1} = \left(\partial \mu_2 / \partial m_1\right)_{T,p,m_2}$ and $\mu_{22}^{(m)} \equiv \left(\partial \mu_2 / \partial m_2\right)_{T,p,m_1}$ are the derivatives of the chemical potentials, μ_1 and μ_2, with respect to the molalities m_1 and m_2, T the absolute temperature, and p is the pressure.

In the following sections, I will report expressions for the chemical potentials for three important cases: 1) neutral macromolecule with neutral additive; 2) neutral macromolecule with salt; 3) charged macromolecule with salt. The first case is the simplest one and will be discussed to introduce basic aspects of preferential interactions. The two-domain model mentioned in Chap 1 will be also presented. The second case

directly applies to my experimental investigation on the PEG(1)-KCl(2)-water system. The third case applies to the previously reported investigation on the lysozyme(1)-KCl(2)-water system. This last case has been included because it will be important for the comparison between the PEG and lysozyme investigations. [13, 21, 57]

Ternary mixture with neutral macromolecule and neutral additive

The chemical potentials of the macromolecule and additive can be written as:

$$\hat{\mu}_1 = \ln m_1 + \beta_1 \qquad (2)$$

$$\hat{\mu}_2 = \ln m_2 + \beta_2 \qquad (3)$$

where $\hat{\mu}_i \equiv (\mu_i - \mu_i^0)/RT$ with $i = 1,2$; R is the ideal-gas constant, and μ_i^0 is the standard chemical potential. In Eqs. 2,3, $\beta_i(m_1, m_2, T, p)$ its a chemical-potential excess. This thermodynamic function is related to the corresponding activity coefficient, γ_i, by $\beta_i = \ln \gamma_i$. For an ideal-dilute solution, $\beta_i = 0$.

The corresponding chemical potential derivatives: $\hat{\mu}_{ij} \equiv (\partial \hat{\mu}_i / \partial m_j)_{m_i, i \neq j, T, p}$ with $i, j = 1,2$ are defined by the following matrix:

$$\begin{bmatrix} \hat{\mu}_{11} & \hat{\mu}_{12} \\ \hat{\mu}_{21} & \hat{\mu}_{22} \end{bmatrix} = \begin{bmatrix} \frac{1}{m_1} + \beta_{11} & \beta_{12} \\ \beta_{21} & \frac{1}{m_2} + \beta_{22} \end{bmatrix} \qquad (4)$$

where $\hat{\mu}_{12} = \hat{\mu}_{21}$. This set of derivatives defines the thermodynamic net interactions between the two solutes. Specifically, the coefficient β_{11} describes macromolecule-macromolecule interactions and β_{22} describe additive-additive interactions. These are directly related to the values of β_{11} and β_{22} of the corresponding solute-solvent binary systems. The coefficient $\beta_{12} = \beta_{21}$ characterizes the macromolecule-additive interaction. Contrary to β_{11} and β_{22}, β_{12} has no direct relation to the solute-solvent binary systems, and it is an important thermodynamic feature of ternary mixtures. A thermodynamic parameter closely related to β_{12} is the preferential-interaction coefficient: $\Gamma_{12} = -\hat{\mu}_{12} / \hat{\mu}_{22}$. Using Eq. 4, we obtain:

$$\Gamma_{12} = \frac{\beta_{12} m_2}{1 + \beta_{22} m_2} \qquad (5)$$

Note that, at low additive concentration, we can approximately write: $\Gamma_{12} \approx \beta_{12} m_2$.

Physical insight on the meaning of Γ_{12} can be obtained by considering the two-domain model. The first domain is represented by the water-additive layer surrounding the macromolecule. This local domain is in chemical equilibrium with a bulk domain, representing the water-additive remaining solution. Figure 1 illustrates the two-domain

model. The black circle represents the macromolecule. The layer surrounding the macromolecule is enclosed inside the dashed circle. This dashed circle represents an imaginary membrane permeable to the additive and solvent molecules. The bulk domain, which has exactly the same properties as the binary additive-solvent system, is represented by the area outside the membrane.[16, 29, 32]

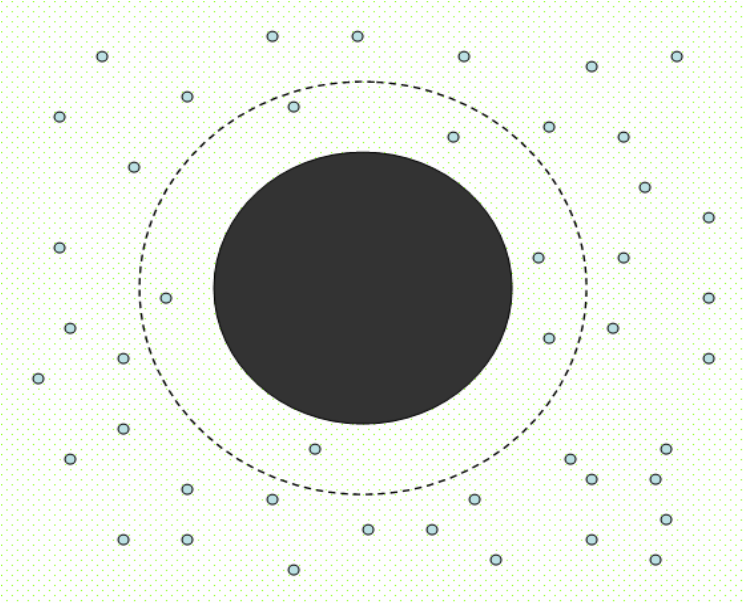

Figure 1

The small dots represent the molecules of the additive, which partition between the local domain and the bulk domain. This chemical equilibrium can be described by introducing the partitioning constant:

$$\alpha = \frac{(N_2 / N_0)}{(n_2^{(b)} / n_0^{(b)})} \tag{6}$$

where N_2 and N_0 are respectively the number of additive and water molecules inside the local domain, and $n_2^{(b)}$ and $n_0^{(b)}$ are respectively the number of additive and water molecules of the bulk domain. When $\alpha < 1$, the additive is preferentially excluded from the local domain. On the other hand, when $\alpha > 1$, the additive preferentially interacts with the macromolecule. A relation can be obtained between α and Γ_{12}. We start by considering the following two mass balances on the total number of molecules, n_2 and n_0,

$$n_2 = N_2\, n_1 + n_2^{(b)} \tag{7}$$

$$n_0 = N_0\, n_1 + n_0^{(b)} \tag{8}$$

where n_1 is the number of macromolecules in solution. Within this model, the preferential-interaction parameter is given by:

$$\Gamma_{12} = \lim_{m_1 \to 0} \left(\frac{\partial m_2}{\partial m_1} \right)_{T,p,\mu_2} = \lim_{m_1 \to 0} \frac{m_2 - m_2^{(b)}}{m_1} = \lim_{m_1 \to 0} \frac{(n_2 / n_0) - (n_2^{(b)} / n_0^{(b)})}{(n_1 / n_0)} \tag{9}$$

Using Eqs. 7,8, we can write:

$$\frac{(n_2 / n_0) - (n_2^{(b)} / n_0^{(b)})}{(n_1 / n_0)} = \frac{n_0}{n_1} \left(\frac{n_2^{(b)} + N_2\, n_1}{n_0^{(b)} + N_0\, n_1} - \frac{n_2^{(b)}}{n_0^{(b)}} \right) = \frac{n_0 (N_2 n_0^{(b)} - N_0 n_2^{(b)})}{(n_0^{(b)} + N_0\, n_1)\, n_0^{(b)}} \tag{10}$$

Using Eq. 6, we can rewrite Eq. 10 in the following way:

$$\frac{(n_2/n_0)-(n_2^{(b)}/n_0^{(b)})}{(n_1/n_0)}=\frac{n_2^{(b)}}{n_0^{(b)}}\frac{n_0\,N_0}{n_0^{(b)}+N_0\,n_1}(\alpha-1) \qquad (11)$$

By taking the limit of $n_1 \to 0$, we also have: $n_0^{(b)} \to n_0$ and $n_2^{(b)} \to n_2$. Since $m_2/m_0 = n_2/n_0$, we finally obtain:

$$\Gamma_{12}=\frac{m_2}{m_0}N_0\,(\alpha-1) \qquad (12)$$

where $m_0 = 55.51 \text{mol kg}^{-1}$. Eq. 12 shows that $\Gamma_{12} < 0$ if the additive is preferentially excluded from the local domain. On the other hand, when $\Gamma_{12} > 0$, the additive preferentially interacts with the macromolecule. Since the solvent is the component present in large excess, N_0 will not significantly change with additive concentration. This implies that Γ_{12} is directly proportional to m_2 within this two domain model, and $\beta_{12} \propto (1+\beta_{22}m_2)$ in Eq. 5. Furthermore it is important to remark that measurements of Γ_{12} as a function of m_2 allow us to determine $N_0\,(\alpha-1)$. However the separate determination of N_0 and α is not possible.

Ternary mixture with neutral macromolecule and 1:1 electrolyte

In this case, the additive is a 1:1 electrolyte (e.g., KCl). The chemical potentials of the macromolecule and additive can be written as:

$$\hat{\mu}_1 = \ln m_1 + \beta_1 \tag{13}$$

$$\hat{\mu}_2 = \ln m_+ + \ln m_- + \beta_2 = 2\ln m_2 + \beta_2 \tag{14}$$

where m_+ and m_- are the cation and anion molalities respectively. The right side of Eq. 14 is obtained from the fact that $m_2 = m_+ = m_-$ for a solution with neutral macromolecules. Note that the difference between the previous case is that a coefficient "2" is introduced in Eq. 14 compared to Eq. 3.

Furthermore, the mean activity coefficient $\gamma_\pm$ is usually reported for salts. This is related to the chemical-potential excess by $\beta_2 = 2\ln\gamma_\pm$.

The corresponding chemical potential derivatives are defined by the following matrix:

$$\begin{bmatrix} \hat{\mu}_{11} & \hat{\mu}_{12} \\ \hat{\mu}_{21} & \hat{\mu}_{22} \end{bmatrix} = \begin{bmatrix} \dfrac{1}{m_1} + \beta_{11} & \beta_{12} \\ \beta_{21} & \dfrac{2}{m_2} + \beta_{22} \end{bmatrix} \tag{15}$$

and the preferential-interaction coefficient is given by

$$-\Gamma_{12} = \frac{\beta_{12}\, m_2}{2 + \beta_{22}\, m_2} \qquad (16)$$

Note that, at low additive concentration, we can approximately write: $\Gamma_{12} \approx (\beta_{12}/2)\, m_2$.

The two-domain model can be also extended to 1:1 electrolytes. The partitioning is still defined using Eq. 6 by assuming however that $N_2 = (N_+ N_-)^{1/2}$ and $n_2^{(b)} = (n_+^{(b)}\, n_-^{(b)})^{1/2}$, where N_+ and N_- are respectively the number of cations and anions inside the local domain, and $n_+^{(b)}$ and $n_-^{(b)}$ are respectively the number of cations and anions of the bulk domain. Figure 2 illustrates the two-domain equilibrium in the presence of two types of ions.

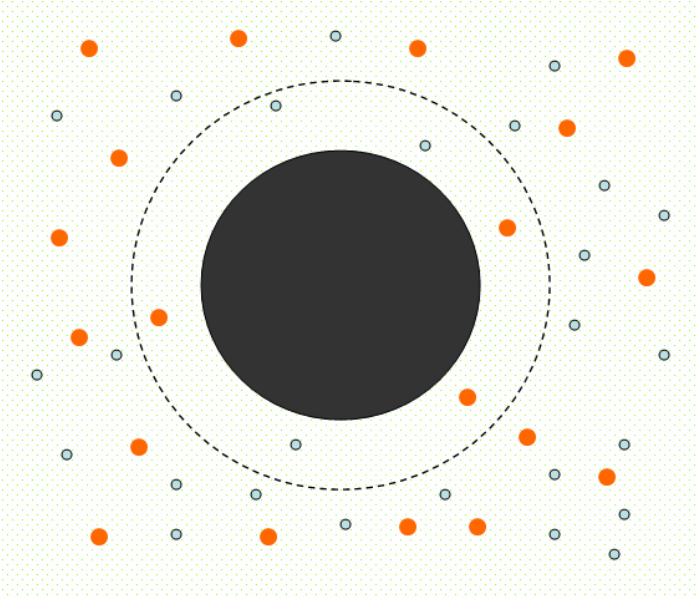

Figure 2

The following two mass balances replace Eq. 7，8:

$$n_+ = N_+ n_1 + n_+^{(b)} \tag{17}$$

$$n_- = N_- n_1 + n_-^{(b)} \tag{18}$$

where n_+ and n_- are the total number of cations and anions respectively. It is important to remark that $n_2 = n_+ = n_-$. However similar equations cannot be applied to the two domains taken separately. In other words, a given local domain may be charged due to preferential binding of one type of ion with respect to the other.

To determine the expression for Γ_{12}, we need to define $n_2^{(b)}$. We first assume that the electrolyte chemical potential, $\hat{\mu}_2^{(b)}$, of the bulk domain is equal to that of an equivalent

binary electrolyte-water solution with molality, $m_2^{(b)} = n_2^{(b)}(m_0 / n_0^{(b)})$ and the same chemical-potential excess, $\beta_2^{(b)}$. We can therefore write:

$$\hat{\mu}_2^{(b)} = \ln m_+^{(b)} + \ln m_-^{(b)} + \beta_2^{(b)} = 2\ln m_2^{(b)} + \beta_2^{(b)} \tag{19}$$

where $m_+^{(b)} = n_+^{(b)}(m_0 / n_0^{(b)})$ and $m_-^{(b)} = n_-^{(b)}(m_0 / n_0^{(b)})$.

From Eq. 19, we obtain the definition of $n_2^{(b)}$:

$$n_2^{(b)} = \left(n_+^{(b)}\, n_-^{(b)}\right)^{1/2} \tag{20}$$

Using Eqs. 4,20, we are now in position to write

$$\frac{(n_2 / n_0) - (n_+^{(b)}\, n_-^{(b)})^{1/2} / n_0^{(b)}}{(n_1 / n_0)} = \frac{n_0}{n_1}\left(\frac{[(n_+^{(b)} + N_+ n_1)(n_-^{(b)} + N_- n_1)]^{1/2}}{(n_0^{(b)} + N_0\, n_1)} - \frac{(n_+^{(b)}\, n_-^{(b)})^{1/2}}{n_0^{(b)}}\right) \tag{20}$$

where we have used Eqs. 8,17,18 and $n_2 = n_+ = n_- = (n_+ n_-)^{1/2}$.

To first order with respect to n_1, we can write:

$$(n_+^{(b)} + N_+ n_1)^{1/2}(n_-^{(b)} + N_- n_1)^{1/2} = \left(n_+^{(b)} n_-^{(b)}\right)^{1/2}\left[1 + \frac{1}{2}\left(\frac{N_+}{n_+^{(b)}} + \frac{N_-}{n_-^{(b)}}\right) n_1\right] \tag{21}$$

Hence, by taking the limit of $n_1 \to 0$ in Eq. 20, we obtain:

$$\Gamma_{12} = \lim_{m_1 \to 0} \frac{(n_2 / n_0) - (n_2^{(b)} / n_0^{(b)})}{(n_1 / n_0)} = \frac{1}{2}(N_+ + N_-) \qquad (22)$$

If we define $N_2 \equiv (1/2)(N_+ + N_-)$ as the apparent number of additive molecules in the local domain, we obtain Eq. 12. Since Γ_{12} is still directly proportional to m_2 , we have $\beta_{12} \propto (2 + \beta_{22} m_2)$ in Eq. 16.

In conclusion, the two-domain model for the electrolyte case shows that anion and cation may have different behavior. For example, a metal ion may preferentially bind to the neutral macromolecule, and the anion may be preferentially excluded from its local domain. Here the preferential-interaction coefficient describes the electrolyte net effect by considering the average N_2 .

Ternary mixture with charged macromolecule and 1:1 electrolyte

In this case, the macromolecule has a charge: z . Here, we will assume that z is positive. The chemical potentials of the macromolecule and additive can be written as:

$$\hat{\mu}_1 = \ln m_1 + z \ln m_- + \beta_1 = \ln m_1 + z \ln \left(z\, m_1 + m_2 \right) + \beta_1 \tag{23}$$

$$\hat{\mu}_2 = \ln m_+ + \ln m_- + \beta_2 = \ln m_2 + \ln \left(z\, m_1 + m_2 \right) + \beta_2 \tag{24}$$

Here, we need to keep in mind the presence of a common ion. Both the charged macromolecule and the electrolyte components contribute to the concentration of the common-ion. For positively charged macromolecules, the common ion is the anion. We therefore have: $m_- = z\, m_1 + m_2$. Correspondingly, the cation becomes the coion, and $m_+ = m_2$.

The corresponding chemical potential derivatives are defined by the following matrix:

$$\begin{bmatrix} \hat{\mu}_{11} & \hat{\mu}_{12} \\ \hat{\mu}_{21} & \hat{\mu}_{22} \end{bmatrix} = \begin{bmatrix} \dfrac{1}{m_1} + \dfrac{z^2}{z\, m_1 + m_2} + \beta_{11} & \dfrac{z}{z\, m_1 + m_2} + \beta_{12} \\ \dfrac{z}{z\, m_1 + m_2} + \beta_{21} & \dfrac{1}{z\, m_1 + m_2} + \dfrac{1}{m_2} + \beta_{22} \end{bmatrix} \tag{25}$$

However, the molality of macromolecules is normally very low compared to that of low-molecular-weight additives. Hence, the condition: $z\ m_1 << m_2$ applies. We can therefore simplify Eq. 25 thereby obtaining:

$$\begin{bmatrix} \hat{\mu}_{11} & \hat{\mu}_{12} \\ \hat{\mu}_{21} & \hat{\mu}_{22} \end{bmatrix} = \begin{bmatrix} \frac{1}{m_1} + \frac{z^2}{m_2} + \beta_{11} & \frac{z}{m_2} + \beta_{12} \\ \frac{z}{m_2} + \beta_{21} & \frac{2}{m_2} + \beta_{22} \end{bmatrix} \qquad (26)$$

where $\beta_{12} = \beta_{21}$. The preferential-interaction coefficient is given by

$$-\Gamma_{12} = \frac{z + \beta_{12} m_2}{2 + \beta_{22} m_2} \qquad (27)$$

Note that, at low additive concentration (and $z\ m_1 << m_2$), we can approximately write:

$$-\Gamma_{12} \approx (z/2) + (\beta_{12}/2)\, m_2 .$$

The two-domain model can be also extended to charged macromolecules in the presence of 1:1 electrolytes. To determine the expression for Γ_{12} we need to define $n_2^{(b)}$ as in the previous case, by considering an equivalent binary electrolyte-water solution with molality, $m_2^{(b)} = n_2^{(b)} (m_0 / n_0^{(b)})$, and the same chemical-potential excess, $\beta_2^{(b)}$. In other words, we can still use Eq. 19 for the definition: $n_2^{(b)} = \left(n_+^{(b)}\, n_-^{(b)} \right)^{1/2}$. Here, however, we

need to keep in mind the common-ion effect. In other words, $n_2 = n_+ = n_- = (n_+ n_-)^{1/2}$ is no longer valid. We now need to find the correct relation between n_2, n_+ and n_-. We first observe that

$$n_2 = n_+ = n_+^{(b)} + N_+ n_1 \tag{28}$$

$$n_2 = n_- - z n_1 = n_-^{(b)} + (N_- - z) n_1 \tag{29}$$

We can therefore write:

$$n_2 = \left(n_+^{(b)} n_-^{(b)}\right)^{1/2} \left[1 + \frac{N_+ n_1}{n_+^{(b)}}\right]^{1/2} \left[1 + \frac{N_- - z}{n_-^{(b)}} n_1\right]^{1/2} \tag{30}$$

To first order with respect to n_1, we obtain:

$$n_2 = \left(n_+^{(b)} n_-^{(b)}\right)^{1/2} \left[1 + \frac{1}{2}\left(\frac{N_+}{n_+^{(b)}} + \frac{N_- - z}{n_-^{(b)}}\right) n_1\right] \tag{31}$$

We are now in position to derive the expression for Γ_{12}

$$\Gamma_{12} = \lim_{m_1 \to 0} \frac{(n_2 / n_0) - (n_2^{(b)} / n_0^{(b)})}{(n_1 / n_0)} = \frac{1}{2}(N_+ + N_- - z) \tag{32}$$

If we define $N_2 \equiv (1/2)(N_+ + N_-)$ as the apparent number of additive molecules in the local domain, we obtain:

$$\Gamma_{12} = -\frac{z}{2} + \frac{m_2}{m_0} N_0 (\alpha - 1) \qquad (33)$$

Contrary to Eq. 12, Γ_{12} in Eq. 33 does not approach zero as $m_2 \to 0$. The intercept $z/2$ characterizes the common-ion effect. It is important to remark that, due to the $z/2$ term, the sign of Γ_{12} is not directly related to partitioning of the electrolyte between the two domains. For example, $\Gamma_{12} < 0$ does not necessarily mean that the electrolyte is preferentially excluded from the local domain. This has been a common error in the literature, where individual values of Γ_{12} have been used for characterizing protein-salt thermodynamic interactions by applying Eq. 12; i.e. $N_0 (\alpha - 1) = \Gamma_{12} (m_0 / m_2)$. For these systems, Eq. 33 must be used, and only measurements of Γ_{12} as a function of m_2 allow us to determine both $N_0 (\alpha - 1)$ and z.

Chapter 3

Multicomponent diffusion

Introduction

When no external forces (e.g., electric or gravitation field) are applied, diffusion is most simply defined as the process whereby an initially non-uniform distribution of species in a mixture proceeds toward a uniform distribution.[1, 2] This macroscopic phenomenon is related to the motion of the molecules within the system, and the higher the particles mobility, the faster is the relaxation towards the equilibrium distribution. In this chapter, we review the fundamental phenomenological equations used for characterizing isothermal diffusion processes for binary and ternary mixtures.

Non-equilibrium thermodynamics provides the basis for the phenomenological description of irreversible processes through the use of three postulates. For an isothermal and isobaric diffusion process, these postulates are:

Postulate 1: *For a system in which irreversible processes are taking place, all thermodynamic functions of state exist for each element of the system.*

Postulate 2: *The fluxes of the system components are linear, homogeneous functions of the chemical-potential gradients, which are thermodynamic driving forces*.

Postulate 3: *If linear equations are written for the set of conjugated thermodynamic forces and fluxes, and if the resulting phenomenological coefficients are well defined, then the matrix of these phenomenological coefficients is symmetric.*

The third postulate is also referred as the *Onsager Reciprocal Relations* (ORR). Lars Onsager received the Nobel Prize in Chemistry in 1968 for providing its microscopic basis. Our use of multicomponent diffusion for extracting preferential-interaction coefficients represents one of the most important applications of the ORR. [1,2,40,58-59]

Binary mixture

The simplest type of diffusion occurs in binary solute(1)-solvent(0) solution. Diffusion is conveniently described by Fick's first law:

$$-J_1 = D_1 \nabla C_1 \qquad (1)$$

Here, C_1 is molar concentration of the solute, J_1 is the corresponding flux and D_1 is called the mutual diffusion coefficient.

However, according to non-equilibrium thermodynamics, the actual driving force is the

gradient of the solute chemical potential, μ_1. Thus, we can write:

$$-J_1 = L_1 \nabla \mu_1 \qquad (2)$$

where L_1 is called the Onsager diffusion coefficient. We can combine Eq. 1 and Eq. 2 together yielding:

$$D_1 = RT\, L_1\, \hat{\mu}_{11}^{(c)} \qquad (3)$$

where $\hat{\mu}_{11}^{(c)} \equiv (\partial \mu_1 / \partial C_1)_{T,p} / RT$. The superscript "(c)" is introduced to indicate that the derivative is taken with respect to the molar concentration. In this way, we can distinguish this type of derivative from those based on molality, which were introduced in Chap. 2. It is important to remark that the diffusion coefficient D_1 does not depend only on the mobility of the particles in solution but also on the system thermodynamic behavior through the factor $\hat{\mu}_{11}^{(c)}$ in Eq. 3. This is one of the reason why diffusion measurements can be used for the determination of thermodynamic quantities.

At infinite dilution, we have: $\hat{\mu}_{11}^{(c)} = 1/C_1$. Thus the infinite-dilution coefficient, D_1^0, is given by

$$D_1^{\,0} = RT \frac{L_1}{C_1} \qquad (4)$$

Since D_1 does not vanish as $C_1 \to 0$, we conclude that $L_1 \propto C_1$.

Brownian-motion theory provides the basis for understanding the physical meaning of D_1^0. The most important result of this theory is the Stokes-Einstein equation:[2]

$$D_1^0 = \frac{k_B T}{6\pi R_h \eta} \qquad (5)$$

where k_B is the Boltzmann constant, R_h is the equivalent hydrodynamic radius, and η is the viscosity of the solvent assumed to be a continuum fluid. Eq. 5 shows that the diffusion coefficients of macromolecules are small compared to that of the small ions or additive molecules. Eq. 5 also shows that D_1^0 decreases as the viscosity of the surrounding continuum fluid increases. This is because viscosity provides a resistance to the motion of the macromolecules in solution.

Another important aspect of diffusion is that it must be described relative to different reference frames. Microscopically, this is related to the fact that the velocity of the molecules can be described only if a given reference frame is introduced. Diffusion coefficients are normally reported with respect to the so-called volume- and solvent-fixed frames. In the volume-fixed frame, the fluxes of the components of a binary system satisfy $(J_0)_V \overline{V}_0 + (J_1)_V \overline{V}_1 = 0$; in the solvent-fixed frame, we have $(J_0)_0 = 0$. Here, J_1 and $\overline{V}_1$ are the molar flux and partial molar volume of the solute, respectively. The

subscript V denotes the volume-fixed frame. The subscript 0 denotes the solvent component when appended directly to a flux, and denotes the solvent-fixed frame when appended outside the parentheses to an already-subscripted flux or diffusion coefficient. Diffusion measurements normally correspond to the volume-fixed frame, $(D_1)_V$. This is because the volume-fixed frame corresponds to the laboratory reference frame to an excellent approximation. The solvent-frame diffusion coefficient $(D_1)_0$ can be calculated by:

$$(D_1)_0 = (D_1)_V /(1 - C_1\bar{V}_1) \qquad (6)$$

Note that, at infinite dilution, we have: $D_1^0 = (D_1)_0 = (D_1)_V$. Generally, we have: $(D_1)_0 > (D_1)_V$. This is because solvent molecules move in the direction opposite to the solute molecules. Thus the mobility of the solute molecules appears relatively higher to an observer at rest with respect to the solvent frame.

Macromolecule(1)-additive(2)-solvent(0) ternary mixtures

In the case of a ternary macromolecule(1)-additive(2)-solvent(0) systems, Fick's first law becomes:[2, 40, 41,60-61]

$$-J_1 = D_{11}\nabla C_1 + D_{12}\nabla C_2 \qquad (7a)$$

$$-J_2 = D_{21}\nabla C_1 + D_{22}\nabla C_2 \qquad (7b)$$

Here, C_1 and C_2 are molar concentrations respectively of macromolecule and additive, J_1 and J_2 are the corresponding fluxes and the four D_{ij}'s (with $i, j = 1, 2$) are the diffusion coefficients. Main-diffusion coefficients, D_{11} and D_{22}, describe the flux of a solute due to its own concentration gradient, while cross-diffusion coefficients, D_{12} and D_{21}, describe the flux of a solute due to the concentration gradient of the other solute. From Eq. 7, we observe that the cross-term D_{ij} with $i \neq j$ vanishes as $C_i \to 0$; otherwise, we have the paradoxical result that $-J_i = D_{ij}\nabla C_j \neq 0$ even in the absence of *i*. The D_{ij} matrix is normally referred as the multicomponent-diffusion matrix.

Also the diffusion coefficients in Eqs. 7 can be described relative to different reference frames.[62] In the volume-fixed frame, the fluxes of the components of a ternary system satisfy $(J_0)_V \overline{V}_0 + (J_1)_V \overline{V}_1 + (J_2)_V \overline{V}_2 = 0$; in the solvent-fixed frame, we have $(J_0)_0 = 0$.

The solvent-fixed frame coefficients, $(D_{ij})_0$, are related to the volume-fixed frame coefficients $(D_{ij})_V$ by the following relation:[63-65]

$$(D_{11})_0 = (D_{11})_V + [C_1/(1 - C_1\bar{V}_1 - C_2\bar{V}_2)]\ [\bar{V}_1(D_{11})_V + \bar{V}_2(D_{21})_V] \quad (8a)$$

$$(D_{12})_0 = (D_{12})_V + [C_1/(1 - C_1\bar{V}_1 - C_2\bar{V}_2)]\ [\bar{V}_1(D_{12})_V + \bar{V}_2(D_{22})_V] \quad (8b)$$

$$(D_{21})_0 = (D_{21})_V + [C_2/(1 - C_1\bar{V}_1 - C_2\bar{V}_2)]\ [\bar{V}_1(D_{11})_V + \bar{V}_2(D_{21})_V] \quad (8c)$$

$$(D_{22})_0 = (D_{22})_V + [C_2/(1 - C_1\bar{V}_1 - C_2\bar{V}_2)]\ [\bar{V}_1(D_{12})_V + \bar{V}_2(D_{22})_V] \quad (8d)$$

The linear laws of non-equilibrium thermodynamics for diffusion in terms of the Onsager diffusion coefficients are simpler in the solvent-fixed frame. In this frame, the fluxes for a ternary system can be written as:

$$-(J_1)_0 = (D_{11})_0\nabla C_1 + (D_{12})_0\nabla C_2 = (L_{11})_0\nabla\mu_1 + (L_{12})_0\nabla\mu_2 \quad (9a)$$

$$-(J_2)_0 = (D_{21})_0\nabla C_1 + (D_{22})_0\nabla C_2 = (L_{21})_0\nabla\mu_1 + (L_{22})_0\nabla\mu_2 \quad (9b)$$

where μ_i is the chemical potential of the *i*-th component, and the $(L_{ij})_0$'s are the Onsager diffusion coefficients in the solvent-fixed frame.[58-59,65-67] The ORR in the solvent-fixed frame is:

$$(L_{12})_0 = (L_{21})_0 \quad (10)$$

We can use Eq. 3 to relate the solvent-fixed diffusion coefficients and $(L_{ij})_0$'s according to:

$$(D_{11})_0 / RT = (L_{11})_0 \hat{\mu}_{11}^{(c)} + (L_{12})_0 \hat{\mu}_{21}^{(c)} \quad (11a)$$

$$(D_{12})_0 / RT = (L_{11})_0 \hat{\mu}_{12}^{(c)} + (L_{12})_0 \hat{\mu}_{22}^{(c)} \quad (11b)$$

$$(D_{21})_0 / RT = (L_{21})_0 \hat{\mu}_{11}^{(c)} + (L_{22})_0 \hat{\mu}_{21}^{(c)} \quad (11c)$$

$$(D_{22})_0 / RT = (L_{21})_0 \hat{\mu}_{12}^{(c)} + (L_{22})_0 \hat{\mu}_{22}^{(c)} \quad (11d)$$

where the $\hat{\mu}_{ij}^{(c)}$'s are defined by $\hat{\mu}_{ij}^{(c)} \equiv (\partial \mu_i / \partial C_j)_{T,p,C_k,k\neq j}$. Eqs. 11 show how the thermodynamic behavior is fundamentally linked to multicomponent-diffusion coefficients. Note that the diffusion cross-terms are different from zero even if $(L_{12})_0 = (L_{21})_0 = 0$. This is because $\hat{\mu}_{12}^{(c)}$ and $\hat{\mu}_{21}^{(c)}$, which characterize the macromolecule-additive thermodynamic interaction is generally different from zero.

Multicomponent diffusion and Preferential-interaction parameters.

The preferential-interaction parameter is described using molality-based chemical potential derivatives (see chap 2). On the other hand, diffusion is described using the corresponding molarity-based derivative (see Eqs. 11). Hence, we report the relations

between the $\hat{\mu}_{ij}^{(c)}$ and the molality-based $\hat{\mu}_{ij}$:[2,65-66]

$$(C_1/m_1)(1-C_1\bar{V}_1-C_2\bar{V}_2)\,\hat{\mu}_{11}^{(c)}=(1-C_2\bar{V}_2)\,\hat{\mu}_{11}+C_2\bar{V}_1\,\hat{\mu}_{12} \qquad (12a)$$

$$(C_1/m_1)(1-C_1\bar{V}_1-C_2\bar{V}_2)\,\hat{\mu}_{12}^{(c)}=(1-C_1\bar{V}_1)\,\hat{\mu}_{12}+C_1\bar{V}_2\,\hat{\mu}_{11} \qquad (12b)$$

$$(C_2/m_2)(1-C_1\bar{V}_1-C_2\bar{V}_2)\,\hat{\mu}_{21}^{(c)}=(1-C_2\bar{V}_2)\,\hat{\mu}_{21}+C_2\bar{V}_1\,\hat{\mu}_{22} \qquad (12c)$$

$$(C_2/m_2)(1-C_1\bar{V}_1-C_2\bar{V}_2)\,\hat{\mu}_{22}^{(c)}=(1-C_1\bar{V}_1)\,\hat{\mu}_{22}+C_1\bar{V}_2\,\hat{\mu}_{21} \qquad (12d)$$

We now solve Eqs. 11(a-d) with respect to $(L_{12})_0$ and $(L_{21})_0$, and obtain:

$$RT(L_{12})_0=\frac{\hat{\mu}_{11}^{(c)}(D_{12})_0-\hat{\mu}_{12}^{(c)}(D_{11})_0}{\hat{\mu}_{11}^{(c)}\hat{\mu}_{22}^{(c)}-\hat{\mu}_{12}^{(c)}\hat{\mu}_{21}^{(c)}} \qquad (13a)$$

$$RT(L_{21})_0=\frac{\hat{\mu}_{22}^{(c)}(D_{21})_0-\hat{\mu}_{21}^{(c)}(D_{22})_0}{\hat{\mu}_{11}^{(c)}\hat{\mu}_{22}^{(c)}-\hat{\mu}_{12}^{(c)}\hat{\mu}_{21}^{(c)}} \qquad (13b)$$

We can then use Eq. 10 and obtain:

$$(D_{12})_0\,\mu_{11}^{(C)}-(D_{11})_0\,\mu_{12}^{(C)}=(D_{21})_0\,\mu_{22}^{(C)}-(D_{22})_0\,\mu_{21}^{(C)} \qquad (14)$$

By inserting Eqs. 12(a-d) into Eq. 14, and solving with respect to $\hat{\mu}_{12}/\hat{\mu}_{22}$, we obtain:

$$\frac{\hat{\mu}_{12}}{\hat{\mu}_{22}}=\frac{(D_{21})_0(1-C_1\bar{V}_1)-(D_{22})_0C_2\bar{V}_1-(\hat{\mu}_{11}/\hat{\mu}_{22})[(D_{12})_0(1-C_2\bar{V}_2)-(D_{11})_0C_1\bar{V}_2]}{(D_{22})_0(1-C_2\bar{V}_2)-(D_{11})_0(1-C_1\bar{V}_1)+(D_{12})_0\,C_2\bar{V}_1-(D_{21})_0C_1\bar{V}_2} \qquad (15)$$

Eq. 15 shows that measurements of multicomponent-diffusion coefficients can be used to determine $\hat{\mu}_{12}/\hat{\mu}_{22}$, provided that $\hat{\mu}_{11}$ and $\hat{\mu}_{22}$ are known. In the limit of small m_1, which is relevant to Γ_{12}, we can calculate $\hat{\mu}_{11}$ from the ideal-dilute relation: $\hat{\mu}_{11}=1/m_1$. Moreover, in the same conditions, $\hat{\mu}_{22}$ becomes the chemical-potential derivative of the binary additive-solvent system. This derivative can be calculated using available activity-coefficient data of the binary system.

We normally perform diffusion measurements on a small, yet finite, concentration of macromolecules. This, in principle, requires a more accurate determination of $\hat{\mu}_{11}$. However, we remark that the accuracy on $\hat{\mu}_{11}$ need not be high. Indeed, a numerical analysis on Eq. 15 show that even a large $\approx 100\%$ error in $\hat{\mu}_{11}$ results in only $\approx 1\%$ error in $\hat{\mu}_{12}$. This is related to the fact that, typically, we have: $(D_{12})_0,(D_{11})_0 << (D_{22})_0,(D_{21})_0$ for macromolecule-additive-solvent systems. Furthermore, we also have $C_1\overline{V}_2 << 1$ because C_1 is small. This implies that $\hat{\mu}_{11}=1/m_1$ is an excellent approximation for relatively low macromolecule concentrations ($\approx 1\%$ by weight), where the error on the estimation of $\hat{\mu}_{11}$ can be as much as $\approx 10\%$.

We also observe that several terms in Eq. 15 contribute only marginally to the value of $\hat{\mu}_{12}/\hat{\mu}_{22}$. Indeed, numerical analysis shows that we can approximately write:

$$\frac{\hat{\mu}_{12}}{\hat{\mu}_{22}} \approx \frac{(D_{21})_0}{(D_{22})_0} - C_2\bar{V}_1 \qquad (16)$$

We therefore conclude that the ratio: $(D_{21})_0/(D_{22})_0$ is essentially a thermodynamic quantity.

To provide physical insight on why multicomponent diffusion can be used to extract the preferential-interaction parameters, we now describe similarities between equilibrium dialysis and ternary diffusion.[31, 34-36] In equilibrium dialysis, a semipermeable membrane separates a compartment containing the protein-salt-water ternary system and the salt-water binary system. At equilibrium, the salt chemical potential is equal in the two compartments and measurements of the salt concentration difference between the two compartments yields $\hat{\mu}_{12}/\hat{\mu}_{22} = -(\partial m_2/\partial m_1)_{\hat{\mu}_2}$. Let us now consider a ternary diffusion experiment where an initial sharp boundary exists between two solutions having different protein concentrations. Since protein diffuses relatively slowly, the salt component (and the solvent) will reach a quasi-equilibrium condition for which $(J_2)_0 \approx 0$. According to first Fick's law, this implies that $(D_{21})_0\nabla C_1 \approx -(D_{22})_0\nabla C_2$ or, equivalently, $-(\partial C_2/\partial C_1)_{\hat{\mu}_2} \approx (D_{21})_0/(D_{22})_0$. Since $-(\partial C_2/\partial C_1)_{\hat{\mu}_2} \approx -(\partial m_2/\partial m_1)_{\hat{\mu}_2} + C_2\bar{V}_1$, we obtain Eq. 16.

Nernst-Hartley Equations

One of our goals is the comparison of the lysozyme-KCl-water system with the PEG-KCl-water system. For charged macromolecules in the presence of electrolytes, the Nernst-Harley (N-H) equations can be used to describe multicomponent diffusion. Since lysozyme is charged, we will report these equations for ternary systems. The N-H equations are expressions for the four diffusion coefficients valid only at infinite dilution. However they provide valuable physical insight also at finite concentrations.[2,40, 49, 68-69]

The N-H equations describe coupled transport of ions, and do not account for thermodynamic nonideality and Onsager-Fuoss electrophoretic effects since they apply at infinite dilution.[40,70] Gosting has derived the N-H equations for solutions with charged macromolecules.[60, 71] Here we report only the results.

For a macromolecule with charge $z > 0$ in the presence of 1:1 electrolyte, we have: [72]

$$D_{11} = D_m \left[1 + \frac{z^2 C_1}{\Delta} \left(D_- - D_m \right) \right] \qquad (17a)$$

$$D_{12} = D_m \frac{z C_1}{\Delta} \left(D_- - D_+ \right) \qquad (17b)$$

$$D_{21} = D_+ \frac{z C_2}{\Delta} \left(D_- - D_m \right) \qquad (17c)$$

$$D_{22} = D_+ \left[1 + \frac{C_1}{\Delta} \left(D_- - D_+ \right) \right] \qquad (17d)$$

where $\Delta = z^2 C_1 D_m + C_+ D_+ + C_- D_-$. Since the N-H equations pertain only at infinite dilution, where the solvent- and volume-fixed frames coincide, the D_{ij} require no reference-frame subscripts. In Eq. 17, D_m, D_+, and D_- are the diffusion coefficients at infinite dilution concentration of macromolecule, salt coion, and counterion (common-ion) respectively, C_+ and C_- are the corresponding concentrations.

For macromolecular systems, we have $z^2 C_1 D_m << C_+ D_+ + C_- D_-$ (consistent with $z^2 C_1 << C_2$), so that, to good approximation in very dilute solutions, the N-H equations become:

$$D_{11} \approx D_m \left[1 + \frac{z^2 C_1}{C_2} \frac{D_- - D_m}{D_+ + D_-} \right] \qquad (18a)$$

$$D_{12} \approx D_m \frac{z C_1}{C_2} \frac{D_- - D_+}{D_+ + D_-} \qquad (18b)$$

$$D_{21} \approx z \frac{D_+ \left(D_- - D_m \right)}{D_+ + D_-} \qquad (18c)$$

$$D_{22} \approx \frac{2 D_+ D_-}{D_+ + D_-} \qquad (18d)$$

where we have also used $C_2 \approx C_+ \approx C_-$.

We now briefly discuss the physical meaning of Eqs. 18. It is important to note that the D_{ij} values are directly related to the charges of the species and to the mobility

differences $D_- - D_m$ and $D_- - D_+$. From Eq. 18a, we see that D_{11} is larger than the infinite-dilution tracer diffusion coefficient of the macromolecule, D_m. A gradient of component 1 gives gradients of macromolecular cations and anions. To preserve electroneutrality, the faster chloride counterions will electrostatically drag the slower macromolecular cations, thereby generating a flux of component 1, corresponding to $D_{11} > D_m$. However, as the concentration of salt (component 2) increases, the counterions will drag macromolecular cations and coions according to their relative concentrations and charges. As C_2 continues to increase, i.e., as $z C_1 / C_2$ decreases, counterions (anions) will overwhelmingly drag coions, so that in this limit the macromolecules will diffuse following its intrinsic mobility D_m. The diffusion coefficient D_{12} is related to the difference in mobilities between counterion and coion as shown in Eq. 18b. In fact, in the presence of a salt gradient, the two ions will try to diffuse with different speed. If the counterion has a higher mobility, it will generate an internal electric field that will try to drag both macromolecule and coion in the same direction and the cross-diffusion coefficient will be positive. On the other hand, if the coion moves faster than the counterion, it will generate an internal electric field that will push the counterion in the same direction but the macroion in the opposite direction (because of the same charge sign) and the cross diffusion coefficient will be negative. Similarly to the D_{11} case, this dragging effect is large at low salt concentration and becomes very small at high salt concentrations. The N-H equation predicts that D_{12} sharply decreases towards zero. The

cross-diffusion coefficient D_{21} will have an analogous justification. However, we need to observe that a macroion will always have a lower mobility than a smaller counterion. Thus, its value is always expected to be positive. Eq. 18d describes salt diffusion. Since the salt component is present in relatively large excess with respect to the macromolecule, D_{22} is the diffusion coefficient of the binary salt-water system. Eq. 18d simply shows that $1/D_{22}$ is the average between $1/D_+$ and $1/D_-$.

For the lysozyme-KCl system, Eqs. 18(a-c) are important for the following two important observations. For macromolecules, we have: $D_+, D_- >> D_m$. In these conditions, we can take the ratio of D_{21} to D_{22} and use Eq. 33 of Chap. 2 to obtain:

$$\frac{D_{21}}{D_{22}} \approx \frac{z}{2} \approx -\Gamma_{12}(0) \qquad (19)$$

In other words, D_{21}/D_{22} is essentially a thermodynamic quantity. For KCl, we have: $D_- \approx D_+$. This implies that $D_{12} \approx 0$ in Eq. 18b. Hence, with respect to D_{12}, any charged macromolecule in the presence of KCl effectively behaves as a neutral macromolecule. Thus the D_{12} values for the PEG case can be directly compared to those for the lysozyme case without considering the effect of the charge.

Chapter 4

Materials and Methods

Materials

Poly(ethylene glycol) (PEG) with average molecular weight ca 20,000 g mol^{-1} and 99% purity was purchased from Aldrich and used without further purification. For PEG, polydispersity has a minor effect on diffusion coefficients, and it is reasonable to approximate that only one monodisperse macromolecule is present. The molecular weight, M_1, for PEG was taken to be 20,000 g mol^{-1} and its density as 1.3 g cm^{-3} for buoyancy corrections. Deionized water was then passed through a four-stage Millipore filter system to provide high purity water for all the experiments. The molecular weight of water, M_0, was taken as 18.015 g cm^{-3}. Mallinckrodt AR KCl with 99.9% purity was dried by heating at 450 °C for seven hours and used without further purification. The molecular weight of KCl, M_2, was taken to be 74.55 g mol^{-1}, and its density as 1.984 g cm^{-3} for buoyancy corrections.

Solution Preparation

All solutions were prepared by mass with appropriate buoyancy corrections. All weighings were performed with a Mettler Toledo AT400 electrobalance. Stock concentrated solutions of PEG were made by mass. An accurate density measurement

was made and used for buoyancy correction.

The two solutions for each diffusion experiment were prepared by mass. For binary PEG-water experiments, precise masses of PEG stock solutions were diluted with pure water to reach the final target PEG concentrations. For binary KCl-water solutions, precise masses of pure salt were added to flasks and diluted with pure water to reach the final target KCl concentrations. For ternary PEG-KCl-water solutions, precise masses of PEG stock solution and pure salt were added to flasks and diluted with pure water to reach the final target PEG and KCl concentrations. The densities of these solutions were measured and the final molar concentrations calculated.

Density Measurements

All solution densities were measured with a Mettler-Paar DMA40 density meter with an RS-232 output to a Apple II+. By time averaging the output, a precision of ±0.00001 g cm^{-3} or better could be achieved. Accuracy is somewhat lower because it is related to the composition uncertainty of the solutions. The temperature of the vibrating tube in the density meter was controlled with water from a large well-regulated water bath whose temperature was 25.00±0.01°C. The solution density d is related to the vibration period T_v of cell tube by the following relation:

$$d = A + B\,T_v^{\,2} \qquad (1)$$

where A, B are two instrumental constants. Two reference periods are needed to be measured for the determination of the instrumental parameters. We have chosen the water (d_{water} =0.997045 g cm^{-3}) and the air (d_{air} = 0.00115 g cm^{-3}) as reference systems. An accurate value of the air density was estimated by a state equation that shows explicit dependence on the pressure, temperature (25.00 °C), and humidity.

Density measurements are used for calculating both molar concentrations and partial molar volumes, $\overline{V}_i \equiv (\partial V / \partial n_i)_{T,p,n_j,i\neq j}$ with $i, j = 0,1,2$. For the diffusion experiments, several solutions with different concentrations are prepared and the final diffusion coefficient values are associated with the average composition. Since the compositions of those solutions exhibit relatively small differences about the mean, linear concentration dependence for the density is usually assumed: [73]

$$d(C_1, C_2) = d(\overline{C}_1, \overline{C}_2) + H_1\,(C_1 - \overline{C}_1) + H_2\,(C_2 - \overline{C}_2) \qquad (2)$$

and the solute partial molar volumes can be then calculated by:[72]

$$\overline{V}_i = \frac{M_i - H_i}{d(\overline{C}_1, \overline{C}_2) - H_1\,\overline{C}_1 - H_2\,\overline{C}_2} \qquad \text{with } i = 1,2 \qquad (3)$$

The solvent partial molar volume $\bar{V}_0 = (1 - \bar{C}_1 \bar{V}_1 - \bar{C}_2 \bar{V}_2) / \bar{C}_0$ can be calculated by applying the following condition:

$$\sum \bar{C}_i \bar{V}_i = 1 \qquad (4)$$

Rayleigh interferometry and the Gosting diffusiometer

The most precise and accurate methods for the determination of the mutual diffusion coefficients are the optical interferometric techniques (the precision of the diffusion coefficient values was estimated to be equal to about 0.1%).[64,71,74-77] Among these techniques, the versatile Rayleigh method was employed for the characterization of the diffusion properties of PEG-KCl-water systems reported in this work.

I will now review the Rayleigh method, together with the fundamental equations employed for the determination of the multicomponent diffusion coefficients. The Rayleigh method yields the one-dimensional profile of the refractive index of a liquid system contained in a cell with rectangular geometry. This refractive index profile, under given initial and boundary conditions can be used for the determination of the diffusion coefficients.

Light generated from a LASER source (see Fig. 1) and emanated from a point (spatial filter) is rendered convergent by a main spherical lens that focuses the slit image to a "camera" plane. Then two coherent beams are generated by two narrow vertical slits positioned between the convergent lens and the cell. One beam goes through the diffusion channel and one through the reference channel. The interference pattern (Young's interference) is then collected on the "camera" plane. The distance between the fringes is determined by the separation of the two slits while the absolute shift of the fringes is proportional to the difference in the optical path between the two beams. If the refractive index is uniform in the diffusion channel along the *Z* direction, the max value of the fringe at the camera plane in the *Y* direction will be independent of *Z*. Thus straight interference vertical lines are produced. If the refractive index inside the diffusion channel changes along the *Z* direction, the position of the maxima will shift along the same direction as a quantity proportional to the shift in the refractive index. Note that, since the rays are deflected by the gradient of refractive index, a system of cylinder lenses is needed to effectively reverse the deflection and focus the cell to the "camera" plane.

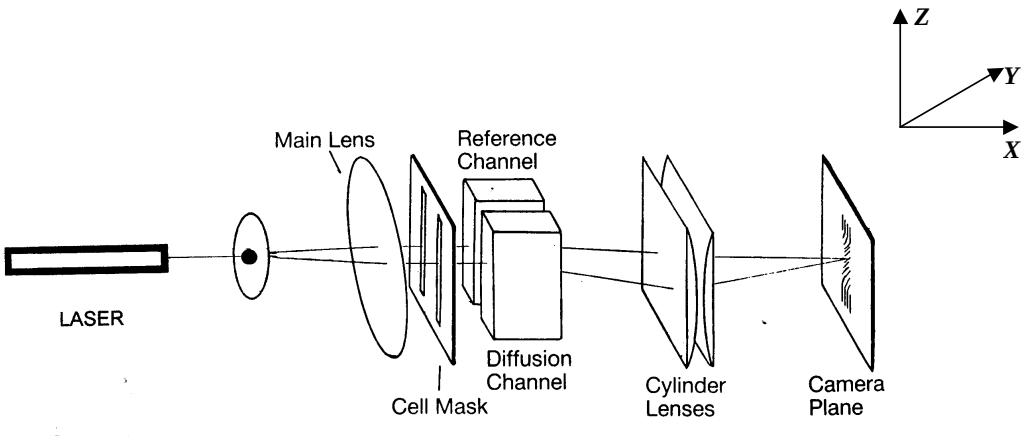

Figure 1: Scheme of the optical apparatus working in Rayleigh configuration.

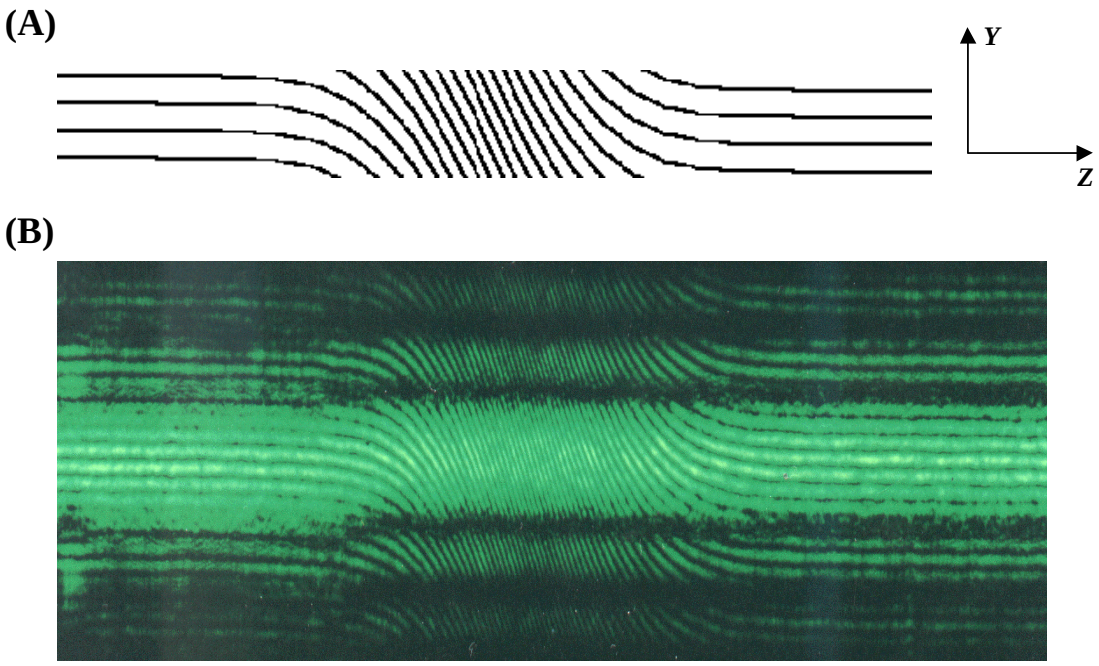

Figure 2: (A) Scheme of the Rayleigh interferometric pattern; the solid lines correspond to maxima positions. (B) Picture of the Rayleigh interferometric pattern taken from the Gosting diffusiometer.

In Fig. 2, I show a picture of a Rayleigh pattern taken from the Gosting diffusiometer operating in the Rayleigh interferometric mode.

The Gosting diffusiometer, located at TCU, is considered to be the best optical diffusiometer in the world. A side view of the diffusiometer (optical-bench length: 8.84 m) is shown in Fig. 3. The light source is a 0.5mW, λ =543.4nm (in air) Uniphase He-Ne LASER. The main lens (focal length: 145.16±0.03 cm) is installed in a lens mount on the source slit side of the water bath so that the diffusion cell is in the converging light between the lens and the camera.[73,77]

The cylinder lens consists of two plane-convex borosilicate lenses, each 7.5 cm square and 1.3 cm thick at its thickest part. A cell holder is used to locate the cell in the bath and to support a mask located between the cell and the light source. The mask consists of a double window allowing the beam to split in two parts, one going through the diffusion channel and the other passing directly in the water bath (reference channel).

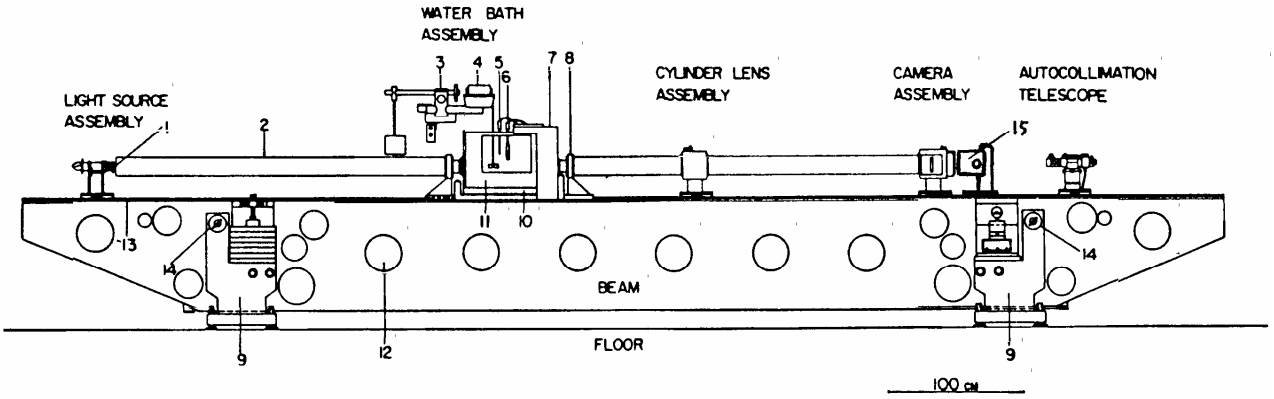

Figure 3: Schematic drawing of the diffusiometer

1. slit of light source
2. tube to minimize air currents in the light path
3. stirring motor mount
4. stirring motor
5. sensor of temperature control
6. heater
7. cell frame support
8. special window rider
9. beam support
10. water bath support
11. water bath
12. access hole to reach the inside of the beam
13. ways
14. leveling collar to check any change in the position of the beam relative to that of beam support
15. digital optical scanner

The cell is a glass Tiselius type. Figure 4 shows the main features of the cell. The cell is composed with three pieces put in contact by very smooth planes surfaces. Grease is used to seal the plates and lubricate sliding relative to each other. The shift of the plates allows the solutions, filled in all three parts, to be either in contact or isolated from each other. The right side of the middle part contains the solution that is then going to be optically investigated (diffusion channel). The reference channel is located on the right side of the diffusion channel. The path length for the cell (model C-1235-H11) employed in the measurements is $l = 2.505_7$ cm.

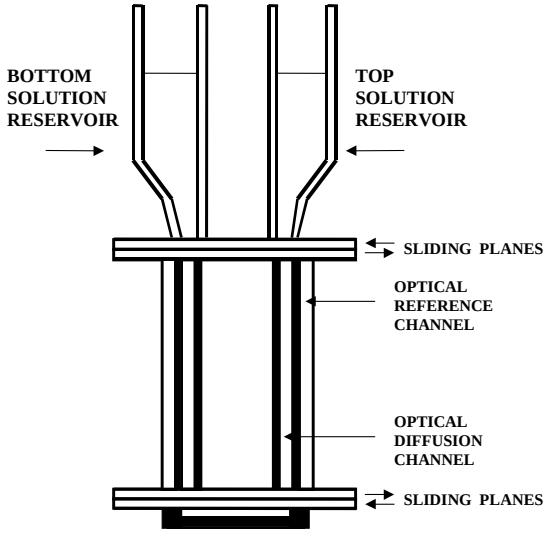

Figure 4: Tiselius cell

The data were recorded from Rayleigh interference patterns by using a vertical linear photodiode array (6 cm long, 6000 pixel, 10x10 μm pixels, model IL-C8-6000-64 with good light sensitivity) that would be moved horizontally through the pattern on precision ways with a stepping motor and a processes screen.

The most important step for a successful experiment is the preparation of a good initial condition from which the diffusion process will be investigated in its evolution. We want to combine the two solutions with different compositions in the diffusion channel. The more dense solution is put in the bottom part of the diffusion channel to avoid convection. The top solution will interface at the center of the cell (at the optic axis) separated by a sharp and flat boundary. A sharp boundary between bottom and top solutions is obtained by lowering a needle into the optic axis of the diffusion channel. The solutions are drawn out of the cell through the needle with a peristaltic pump. When sufficient time has elapsed after the needle is removed, diffusion patterns clearly emerge which can be resolved by the optical scanner. A set of diffusion scans (usually 50), equally distributed in time are performed. The refractive index profile along the vertical Z direction is then extracted. However, the projection of the cell onto the camera plane results in magnification, and conversion to the cell dimension is necessary. The magnification factor can be easily evaluated by projecting a grating scale located in the cell holder onto the camera plane.

The refractive index change as a function of time and position is conveniently defined by the function: $f(j) \equiv (2j - J)/J$, where j is a continuous variable with values ranging between 0 and the total number of fringes J. This function has the property to be equal to zero at the center of the pattern and equal to respectively -1 and +1 at the boundaries. Well-established time-correction and antisymmetrization procedures (Creeth-pair

method)[78] are applied to $f(j)$ in order to remove boundary imperfections, lens aberration and concentration-dependence of diffusion coefficients. I now briefly describe how to extract diffusion coefficients for binary and ternary solutions from $f(j)$.[64, 73, 77]

Extraction of diffusion coefficients from Rayleigh interferometry

For a binary system, we can solve second's Fick's law with the free-diffusion boundary condition and obtain:[49]

$$f(j) = \text{erf}\left(\frac{x}{2\sqrt{t\,D}}\right) \qquad (5)$$

where x is the position (the vertical distance from the solutions initial boundary and parallel to the Z direction of the apparatus in Fig. 1), t is time, D is the diffusion coefficient, and $\text{erf}(z) = \frac{2}{\sqrt{\pi}}\int_0^z e^{-z'^2}\,dz'$. For each x, t and $f(j)$, a value of D is obtained using Eq. 5. The final value of the diffusion coefficient is calculated by taking the average of all D values.[41, 49]

For a ternary system, we can solve Fick's second law with the free-diffusion boundary condition and obtain:

$$f(j) = \Gamma_1 \operatorname{erf}\left(\frac{x}{2\sqrt{t\,\Lambda_1}}\right) + \Gamma_2 \operatorname{erf}\left(\frac{x}{2\sqrt{t\,\Lambda_2}}\right) \qquad (6)$$

where Λ_1 and Λ_2 are the eigenvalues of the matrix of four diffusion coefficients. In Eq. 6, we have

$$\Gamma_1 = a + b\,\alpha_1 \qquad (7a)$$

$$\Gamma_2 = 1 - a - b\,\alpha_1 \qquad (7b)$$

where $\alpha_i = \frac{R_i}{\Delta n}\Delta C_i$, $R_i \equiv (l/\lambda)(\partial n/\partial C_i)_{T,p,C_j,i\neq j}$, n is the refractive index, Δn is the difference in refractive index between bottom and top solution, λ is the laser wavelength, l is the cell path length, ΔC_i is the difference in molar concentration of component i between bottom and top solution, and a and b are two parameters to be determined. The values of R_1 and R_2 are obtained by applying the method of linear least squares to the experimental total number of fringes J plotted against $(\Delta C_1, \Delta C_2)$ using

$$J = R_1 \Delta C_1 + R_2 \Delta C_2 \qquad (8)$$

The quantity α_1 (or $\alpha_2 = 1 - \alpha_1$) defines the initial condition of an individual experiment. To determine a and b, at least two experiments at different α_i need to be

performed. Typically four experiments are performed to reduce measurement error. The non-linear least squares method is applied to $f(j)$ with respect to the independent variables $x/\sqrt{t}$ and α_1 yielding Λ_1, Λ_2, a and b. The ternary diffusion coefficients can be then determined by the following set of equations:

$$D_{11} = \frac{\Lambda_1\Lambda_2}{b}\left[(a+b)(1-a)/\Lambda_2 - a(1-a-b)/\Lambda_1\right] \qquad (9a)$$

$$D_{12} = -\frac{R_2}{R_1}\frac{\Lambda_1\Lambda_2}{b}(1/\Lambda_1 - 1/\Lambda_2)a(1-a) \qquad (9b)$$

$$D_{12} = -\frac{R_1}{R_2}\frac{\Lambda_1\Lambda_2}{b}(1/\Lambda_1 - 1/\Lambda_2)(a+b)(1-a-b) \qquad (9c)$$

$$D_{22} = \frac{\Lambda_1\Lambda_2}{b}\left[(a+b)(1-a)/\Lambda_1 - a(1-a-b)/\Lambda_2\right] \qquad (9d)$$

Finally, we observe that a pseudo-binary diffusion coefficient, D_A, can be determined for individual experiments (with a given α_1) on ternary systems. This can be calculated using: [64]

$$\frac{1}{\sqrt{D_A}} = \frac{\Gamma_1}{\sqrt{\Lambda_1}} + \frac{\Gamma_2}{\sqrt{\Lambda_2}} = \frac{a+b\alpha_1}{\sqrt{\Lambda_1}} + \frac{1-a-b\alpha_1}{\sqrt{\Lambda_2}} \qquad (10)$$

When the concentration gradient of the bottom and top solutions is small, the mixing volume change ΔV_{mix} is also small. We can then assume the laboratory frame as the volume fixed frame, thus $D_{ij} = (D_{ij})_v$

The Isopiestic Method

Chemical-potential derivatives can be obtained using equilibrium techniques such as the isopiestic method.[79-83] This is the most convenient for involatile solutes in a volatile solvent. In this method, mixtures of known weight and composition are located inside open cups of inert metal (eight tantalum cups in our case) which are then placed in a copper block inside a desiccator. The desiccator is then evacuated and then placed in a thermostatted water bath. The solutions are allowed to reach equilibrium as the solvent redistributes itself amongst the mixtures. This equilibration process normally takes a time ranging from one to four weeks.

After equilibrium has been reached, the chemical potential of the solvent is equal in all mixtures inside the desiccator. We will use this property for designing experiments aimed at the determination of preferential-interaction parameters in the case of macromolecule-salt-water ternary mixtures. To my knowledge, this is the first time the isopiestic method has been used for the determination of Γ_{12}.

For each experiment, a given binary KCl-water solution with known composition was prepared by weight and split into two solutions. A known amount of solid PEG was added to one of them. Clearly, the prepared ternary PEG-KCl-water mixture with known composition has the same KCl molality as the initial binary solution. Four amounts of

binary KCl-water solutions and four amounts of ternary PEG-KCl-water solutions were placed inside eight tantalum cups. The weights of the eight solutions were obtained by first measuring the mass of each empty cup. Adding approximately one gram of solution in each cup and immediately placing a pre-weighed cap with an o-ring seal was immediately placed on the cup. The assembled cap and the solution was weighed to 0.1 mg and the mass of solution calculated. The caps were removed and the cups were placed in the apparatus and equilibrated. When the chambers were opened to remove the cups, the set of pre-weighed eight caps were simultaneously pushed onto the cups using a special cup holder. The cups with solutions were then lifted out of the copper block and weighed to 0.1 mg. Final molal concentrations were calculated from weight changes and initial concentrations, here the mass of the cups are assumed no change.

For the four binary KCl-water mixtures, the average KCl molality, m_2', was determined. For the four ternary PEG-KCl-water solutions, the average PEG molality, m_1, and the average KCl molality, m_2. We have then computed

$$\left(\frac{\Delta m_2}{\Delta m_1}\right)_{\mu_0=\mu_0'} = \frac{m_2 - m_2'}{m_1} \qquad (10)$$

where μ_0' is the water chemical potential of the binary solution and μ_0 is the water chemical potential of the ternary solution. Measurements of $\left(\Delta m_2 / \Delta m_1\right)_{\mu_0=\mu_0'}$ at several

m_1, and their extrapolations to $m_1 = 0$ allow us to determine $\left(\partial m_2 / \partial m_1\right)_{\mu_0}$ at $m_1 = 0$. In this conditions, a constant μ_0 implies a constant μ_2 due to Gibbs-Duhem equation. Hence $\Gamma_{12} = \left(\partial m_2 / \partial m_1\right)_{\mu_2} = \left(\partial m_2 / \partial m_1\right)_{\mu_0}$.

Chapter 5

Results

Introduction

In this chapter, I will report the measurements of ternary diffusion coefficients for the PEG(1)-KCl(2)-water(0) system at 25 ºC. Specifically, diffusion measurements were performed at constant PEG concentration (0.25 mM) and as a function of salt concentration (from 0.2 M to 2.3 M). At this low PEG concentration, ternary diffusion coefficients were used to extract preferential-interaction coefficients as a function salt concentration. For comparison, the corresponding binary diffusion coefficients for the PEG-water system and the KCl-water system are also included. Isopiestic measurements were also performed for the PEG-KCl-water system at 25 ºC. The isopiestic results were used to compute the preferential-interaction coefficients at 0.25 M and 1.00 M KCl. These values were found to be in very good agreement with those extracted from the diffusion coefficients.

Diffusion Coefficients

In Table 1, I report experimental parameters related to the diffusion experiments for the ternary PEG(1)-KCl(2)-water(0) system at seven mean KCl concentrations $\bar{C}_2$ = 0.20, 0.25, 0.30, 0.50, 1.00, 2.00 and 2.30 M, and the same mean PEG concentration of

$\bar{C}_1 = 0.25$ mM. In the same table, we also report experimental parameters related to the binary PEG(1)-water(0) system at the same mean PEG concentration. In the Appendix, I have reported experimental details related to individual ternary diffusion experiments and binary experiments on the KCl-water system. In Table 1A, I report the mean density: $d(\bar{C}_1, \bar{C}_2)$, and the two density slopes: H_1 and H_2 of Eq. 2 in Chap. 4. The values were obtained by applying the method of linear least squares to density data using this equation. The corresponding partial molar volumes: $\bar{V}_1$, $\bar{V}_2$ and $\bar{V}_0$ were obtained using Eqs. 3,4 of Chap. 4. The values of R_1 and R_2 describe the dependence of the refractive index on PEG and KCl concentrations respectively (see Chap. 4). These values are obtained using Eq. 8 of Chap. 4. In Table 1B, I report the volume-frame diffusion coefficients $(D_{ij})_{\mathrm{V}}$ and the corresponding eigenvalues, Λ_1 , Λ_2. These parameters were obtained by applying the method of the non-linear least square as described in Chap. 4. In Table 1C, I report the solvent-frame diffusion coefficients $(D_{ij})_0$ obtained from the $(D_{ij})_{\mathrm{V}}$ and $\bar{V}_i$ using Eqs. 8a-8d of Chap. 3. I also report $(D_{11})_0(\eta/\eta_0)$, where η is the viscosity of the corresponding binary KCl-water systems and η_0 is the viscosity of water. The relative viscosity was calculated using the equation: [84]

$$\eta/\eta_0 = 1 + 0.0051\, C_2^{1/2} - 0.0155 C_2 + 0.00772\, C_2^{\,2} \qquad 0 \le C_2 \le 3.5\,\mathrm{M} \qquad (1)$$

The reported values of $\hat{\mu}_{11}$ were calculated assuming ideal-dilute behavior, using: $\hat{\mu}_{11} = 1/m_1$. The reported values of $\hat{\mu}_{22}$ were calculated from the available activity-coefficient data. Specifically, $\hat{\mu}_{22}$ was calculated using:[51]

$$\hat{\mu}_{22} = \frac{2}{m_2}\left(0.94649 - 0.16845 C_2^{1/2} + 0.12744 C_2\right) \qquad 0.1\,\mathrm{M} \le C_2 \le 3.0\,\mathrm{M} \qquad (2)$$

Table 1A. Ternary Diffusion Data for PEG – KCl – H_2O at 25 °C (PART A)

Series ID $\Rightarrow$	0.00 M KCl pkc0	0.20 M KCl pkc6	0.25 M KCl pkc4	0.30 M KCl pkc5	0.50 M KCl pkc2	1.00 M KCl pkc1	2.00 M KCl pkc3	2.30 M KCl pkc7
$\bar{C}_1\,(\mathrm{mM})$	0.2500	0.2500	0.2500	0.2500	0.2500	0.2500	0.2500	0.2500
$\bar{C}_2\,(\mathrm{M})$	0.0000	0.2000	0.2500	0.3000	0.5000	0.9998	2.0000	2.2996
$d(\bar{C}_1,\bar{C}_2)\,(\mathrm{g\ cm^{-3}})$	0.997871	1.007247	1.009553	1.011872	1.021060	1.043622	1.087522	1.100414
$H_1\,(10^3\,\mathrm{g\ mol^{-1}})$	3.311	3.284	3.282	3.292	3.250	3.193	3.074	3.036
$H_2\,(10^3\,\mathrm{g\ mol^{-1}})$	–	0.04646	0.04640	0.04628	0.04578	0.04471	0.04324	0.04289
$\bar{V}_0\,(\mathrm{cm^3\,mol^{-1}})$	0.01807	0.01807	0.01807	0.01807	0.01806	0.01805	0.01801	0.01800
$\bar{V}_1\,(\mathrm{cm^3\,mol^{-1}})$	16.74	16.76	16.77	16.76	16.79	16.84	16.92	16.95
$\bar{V}_2\,(\mathrm{cm^3\,mol^{-1}})$	-	0.02819	0.02824	0.02836	0.02885	0.02991	0.03131	0.03164
$R_1\,(10^2\,\mathrm{dm^3\,mol^{-1}})$	123500	123500	123500	123500	123300	122600	121400	120900
$R_2\,(10^2\,\mathrm{dm^3\,mol^{-1}})$	-	455.7	452.9	450.8	443.1	427.1	402.9	394.7

Table 1B. Ternary Diffusion Data for PEG – KCl – H_2O at 25 °C (PART B)

Series ID $\Rightarrow$	0.00 M KCl pkc0	0.20 M KCl pkc6	0.25 M KCl pkc4	0.30 M KCl pkc5	0.50 M KCl pkc2	1.00 M KCl pkc1	2.00 M KCl pkc3	2.30 M KCl pkc7
$\bar{C}_1\,(\mathrm{mM})$	0.2500	0.2500	0.2500	0.2500	0.2500	0.2500	0.2500	0.2500
$\bar{C}_2\,(\mathrm{M})$	0.0000	0.2000	0.2500	0.3000	0.5000	0.9998	2.0000	2.2996
$\Lambda_1\,(10^{-9}\,\mathrm{m^2 s^{-1}})$	0.05990	0.05962	0.05960	0.06014	0.06010	0.06042	0.06016	0.06002
$\Lambda_2\,(10^{-9}\,\mathrm{m^2 s^{-1}})$	-	1.805	1.809	1.805	1.817	1.861	1.967	2.001
$(D_{11})_v\,(10^{-9}\,\mathrm{m^2 s^{-1}})$	0.05990 ± 0.00004	0.06010 ± 0.00004	0.06016 ±0.00007	0.06082 ±0.00003	0.06107 ±0.00012	0.06230 ±0.00010	0.06356 ±0.00016	0.06393 ±0.00020
$(D_{12})_v\,(10^{-12}\,\mathrm{m^2 s^{-1}})$	-	0.000056 ±0.000001	0.000056 ±0.000002	0.000056 ±0.000001	0.000053 ±0.000003	0.000056 ±0.000002	0.000054 ±0.000002	0.000055 ±0.000003
$(D_{21})_v\,(10^{-9}\,\mathrm{m^2 s^{-1}})$	0	14.7±0.1	17.4±0.2	21.2±0.1	32.2±0.3	61.0±0.2	119.0±0.9	137.9±0.6
$(D_{22})_v\,(10^{-9}\,\mathrm{m^2 s^{-1}})$	-	1.804±0.001	1.809±0.002	1.804±0.005	1.816±0.002	1.859±0.001	1.963±0.002	1.997±0.002

Table 1C. Ternary Diffusion Data for PEG – KCl – H_2O at 25 °C (PART C)

Series ID $\Rightarrow$	0.00 M KCl pkc0	0.20 M KCl pkc6	0.25 M KCl pkc4	0.30 M KCl pkc5	0.50 M KCl pkc2	1.00 M KCl pkc1	2.00 M KCl pkc3	2.30 M KCl pkc7
$\bar{C}_1\,(\mathrm{mM})$	0.2500	0.2500	0.2500	0.2500	0.2500	0.2500	0.2500	0.2500
$\bar{C}_2\,(\mathrm{M})$	0.0000	0.2000	0.2500	0.3000	0.5000	0.9998	2.0000	2.2996
$(D_{11})_0\,(10^{-9}\,\mathrm{m^2 s^{-1}})$	0.06015	0.06010	0.06048	0.06121	0.06160	0.06304	0.06489	0.06537
$(D_{12})_0\,(10^{-9}\,\mathrm{m^2 s^{-1}})$	-	0.000070	0.000069	0.000069	0.000066	0.000070	0.000071	0.000072
$(D_{21})_0\,(10^{-9}\,\mathrm{m^2 s^{-1}})$	0	14.7	17.8	21.6	33.2	64.0	129.3	151.5
$(D_{22})_0\,(10^{-9}\,\mathrm{m^2 s^{-1}})$	-	1.804	1.822	1.820	1.843	1.919	2.097	2.162
$(D_{11})_0\,(\eta/\eta_0)\,(10^{-9}\,\mathrm{m^2 s^{-1}})$	0.06015	0.06042	0.06049	0.06116	0.06143	0.06288	0.06531	0.06625
$\hat{\mu}_{11}\,(\mathrm{mol^{-1} kg})$	3991	3949	3944	3938	3915	3857	3738	3697
$\hat{\mu}_{22}\,(\mathrm{mol^{-1} kg})$	-	8.853	7.052	5.858	3.489	1.746	0.899	0.791
$-\Gamma_{12}$	-	5.1±0.2	5.7±0.2	7.1±0.2	10.0±0.3	17.4±0.2	30.2±0.6	34.3±0.4

Finally, the reported values of $-\Gamma_{12} = \hat{\mu}_{12} / \hat{\mu}_{22}$ were calculated using Eq. 15 of Chap. 3.

In Figs. 1-4, I illustrate the behavior of the four $(D_{ij})_V$ as a function of salt concentration. In Fig. 1, we observe that $(D_{11})_V$ increases with C_2. It is important to remark that the opposite salt-dependence is usually observed for the diffusion coefficient of macromolecules. This interesting result will be discussed in Chap. 6.

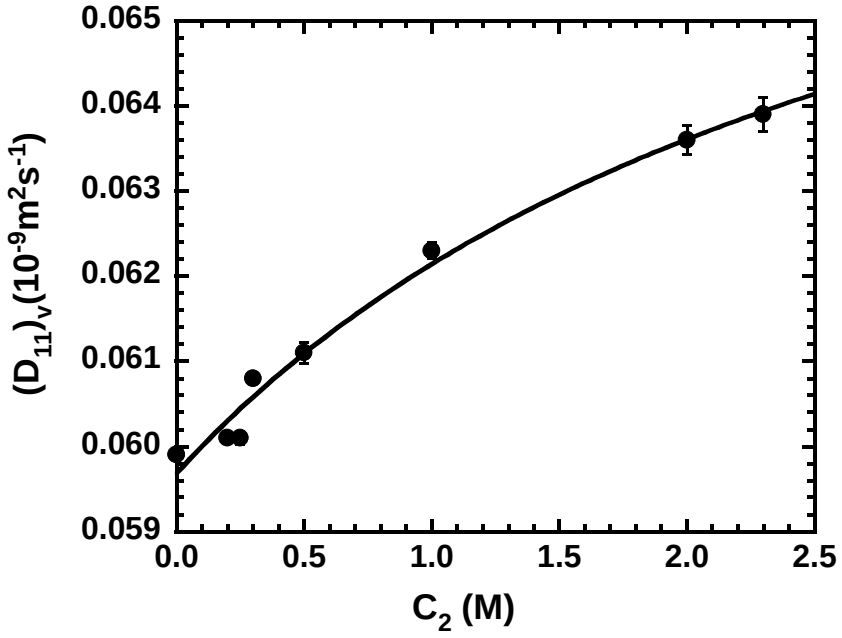

Figure 1. $(D_{11})_V$ as a function of KCl concentration, C_2. The solid curve is a quadratic fit through the data.

In Fig. 2, we observe that $(D_{12})_V$ is essentially independent of C_2 within the experimental error. By linear extrapolation of $(D_{12})_V$ to $C_2 = 0$, we obtain the limiting value: $(D_{12})_V = (0.000056 \pm 0.000001)\ 10^{-9}\,\mathrm{m^2 s^{-1}}$.

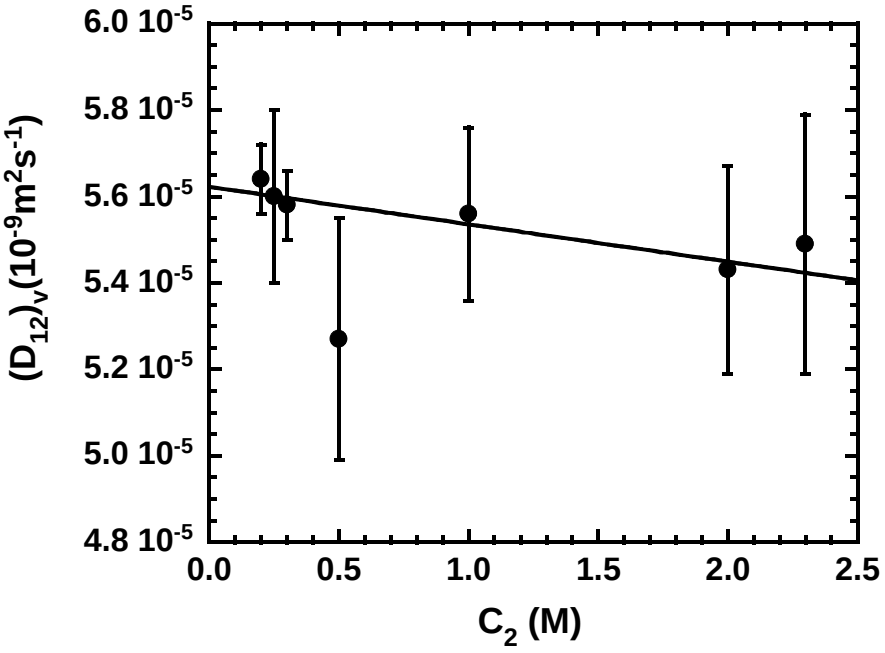

Figure 2. $(D_{12})_V$ as a function of KCl concentration, C_2. The solid line is a weighed linear fit through the data.

In Fig. 3, we observe that $(D_{21})_V$ increases with C_2. Contrary to $(D_{12})_V$, the value of $(D_{21})_V$ must approach zero at $C_2 = 0$. This is because a PEG concentration gradient cannot induce salt diffusion in the absence of salt.

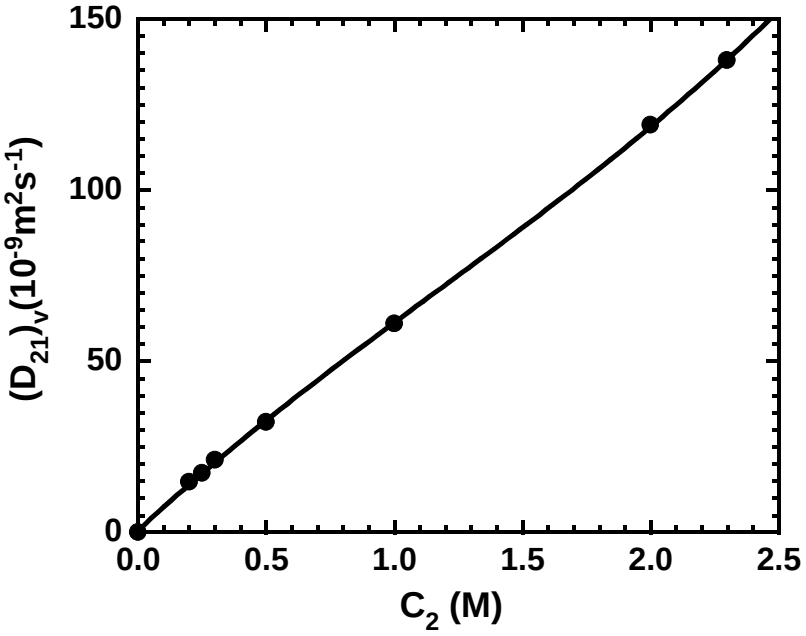

Figure 3. $(D_{21})_V$ as a function of KCl concentration, C_2. The solid curve is a cubic fit through the data.

In Fig. 4, I show the behavior of the salt main-diffusion coefficient $(D_{22})_{\mathrm{V}}$ (solid circles). In the same figure, I also include the corresponding binary diffusion coefficients (open circles) and the literature data (dashed curve) represented by the equation: [73]

$$\left(D_2\right)_{\mathrm{V}} = \left(1.9288 - 0.3966\,C_2^{\,1/2} + 0.5039\,C_2 - 0.1699\,C_2^{\,3/2} + 0.0264C_2^{\,2}\right) 10^{-9}\,\mathrm{m^2 s^{-1}} \qquad (3)$$
$$0 \le C_2 \le 3.0\,\mathrm{M}$$

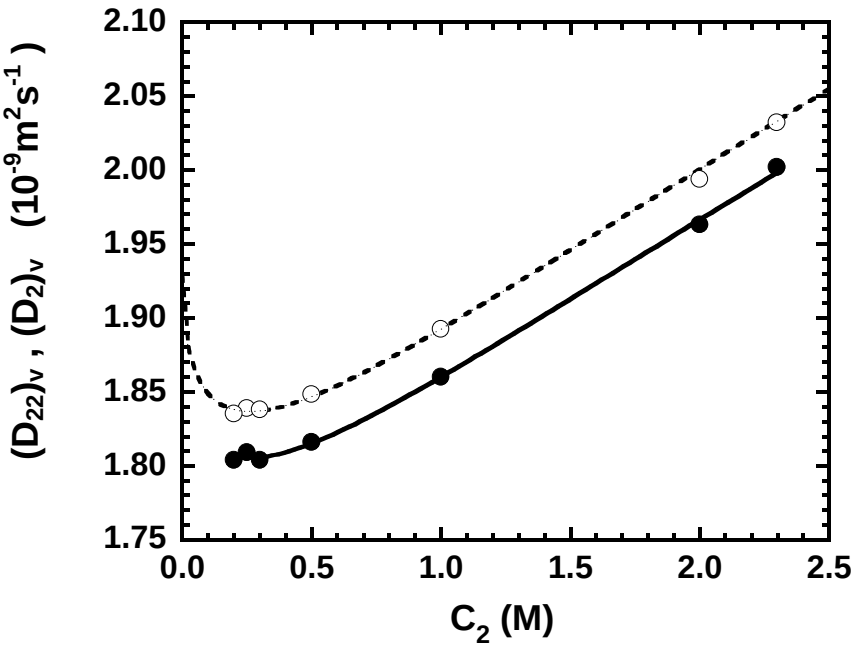

Figure 4. $(D_{22})_{\mathrm{V}}$, ternary diffusion coefficients (solid circles) and $(D_2)_{\mathrm{V}}$, corresponding binary diffusion coefficients (open circles) as functions of KCl concentration C_2. The dashed curve represents Eq. 3. The solid curve is a fit through the ternary data using Eq. 3 and $\xi = 0.983$.

From this figure, we can see that our binary measurements are in very good agreement with literature data as expected. Our ternary data show the same behavior as the corresponding binary curve. Since $(D_{22})_V$ strongly depends on μ_{22}, the equal behavior of these two set of data is strong evidence that using binary thermodynamic data to calculate ternary $\hat{\mu}_{22}$ values is an excellent approximation. Fig. 4 also suggests that ternary data can be related to the corresponding binary data by $(D_{22})_V = \xi (D_2)_V$, where $\xi < 1$ is a constant factor that characterizes an expected small obstruction effect of the PEG macromolecules on the motion of the small salt ions. We have fitted the experimental $(D_{22})_V$ values using $(D_{22})_V = \xi (D_2)_V$, where $(D_2)_V$ is given by Eq. 3. This has allows us to obtain: $\xi = 0.983 \pm 0.001$.

Preferential-Interaction Coefficients

Thermodynamic properties are typically determined from measurements in equilibrium experiments. However, as we have shown in Chap. 4, that need not be the case. Ternary diffusion coefficients can be also used to determine thermodynamic parameters. It is important to observe that the key reason we can determine thermodynamic properties is that the ratios of cross-term to main-term diffusion coefficients are directly related to the system thermodynamics. This is a unique feature of ternary diffusion coefficients, since a similar approach cannot be applied to binary diffusion coefficients.

I also observe that the high precision of the diffusion coefficients achieved using the Gosting diffusiometer allows us to obtain preferential-interaction coefficients with high precision compared to currently employed equilibrium techniques such as dialysis and vapor pressure osmosis. It is however important to remember that the use of non-equilibrium methods for the determination of equilibrium properties may pose some concern about the accuracy of the obtained values. For this reason, I have also used the isopiestic method for the determination of the preferential-interaction coefficients. I want to point out that normally the isopiestic method has been used for the determination of activity coefficients of electrolyte mixtures. To my knowledge, this is the first time that the isopiestic method has been used for the determination of preferential-interaction coefficients of macromolecules.

Although, the isopiestic method is known to provide accurate thermodynamic data, it is also known that isopiestic measurements are time consuming. Indeed, a single measurement may last any time ranging from one to four weeks, whereas a single diffusion measurement normally takes less than six hours which is, for example, typically good for metastable state measurements. Long time isopiestic experiment may be a problem for complex biological macromolecules such as proteins, which may undergo oxidative processes or degradation (due to traces of proteases) during experiment. However, we expect PEG to be relatively more stable than proteins. Thus, our choice of PEG for this comparison is also motivated by the possibility to perform a reliable comparison between diffusion and isopiestic measurements.

In Table 2, measurements of $(\Delta m_2 / \Delta m_1)_{\mu_0=\mu_0'}$ are reported (see Chap. 4) for two chosen KCl concentrations: $C_2 =$ 0.25 and 1.0 M. In the Appendix, I have reported experimental details related to individual isopiestic experiments. In Fig. 5, I plot $-(\Delta m_2 / \Delta m_1)_{\mu_0=\mu_0'}$ as a function of m_1 at both salt concentrations. These two sets of data were fitted using the linear weighed least squares method. The corresponding intercepts are the values of $-\Gamma_{12}$. I obtain: $-\Gamma_{12} = 5.2 \pm 0.4$ at $C_2 =$ 0.25 M, and $-\Gamma_{12} = 16.6 \pm 0.7$ at $C_2 =$ 1.0 M, where the reported errors are standard deviations. The corresponding values obtained using ternary diffusion coefficients are: $-\Gamma_{12} = 5.7 \pm 0.2$ and $-\Gamma_{12} = 17.4 \pm 0.2$ (from Table 1). We therefore conclude that diffusion and isopiestic measurements are in very good agreement within the experimental error.

Table 2A. Isopiestic Data for PEG – KCl – H_2O at KCl 0.25 M and 25 °C

$\bar{m}_1$ (mol Kg^{-1})	$\bar{m}_2$ (mol Kg^{-1})	$\bar{m}'_2$ (mol Kg^{-1})	$(\Delta m_2 / \Delta m_1)_{\mu_0=\mu'_0}$
0.2131	0.2676	0.2664	-5.5±3.1
0.4233	0.2668	0.2644	-5.5±0.4
0.6370	0.2684	0.2649	-5.4±0.2
0.7861	0.2656	0.2616	-5.1±0.5
1.0242	0.2614	0.2564	-4.8±0.5
1.2970	0.2671	0.2599	-5.5±0.3

Table 2B. Isopiestic Data for PEG – KCl – H_2O at KCl 1.0 M and 25 °C

$\bar{m}_1$ (mol Kg^{-1})	$\bar{m}_2$ (mol Kg^{-1})	$\bar{m}'_2$ (mol Kg^{-1})	$(\Delta m_2 / \Delta m_1)_{\mu_0=\mu'_0}$
0.2634	1.0575	1.0533	-15.8±1.8
0.5432	1.0757	1.0757	-17.2±1.1
0.7801	1.0517	1.0398	-15.2±1.1
1.1163	1.0139	0.9952	-16.8±0.4
2.3566	0.9763	0.9369	-16.7±0.7

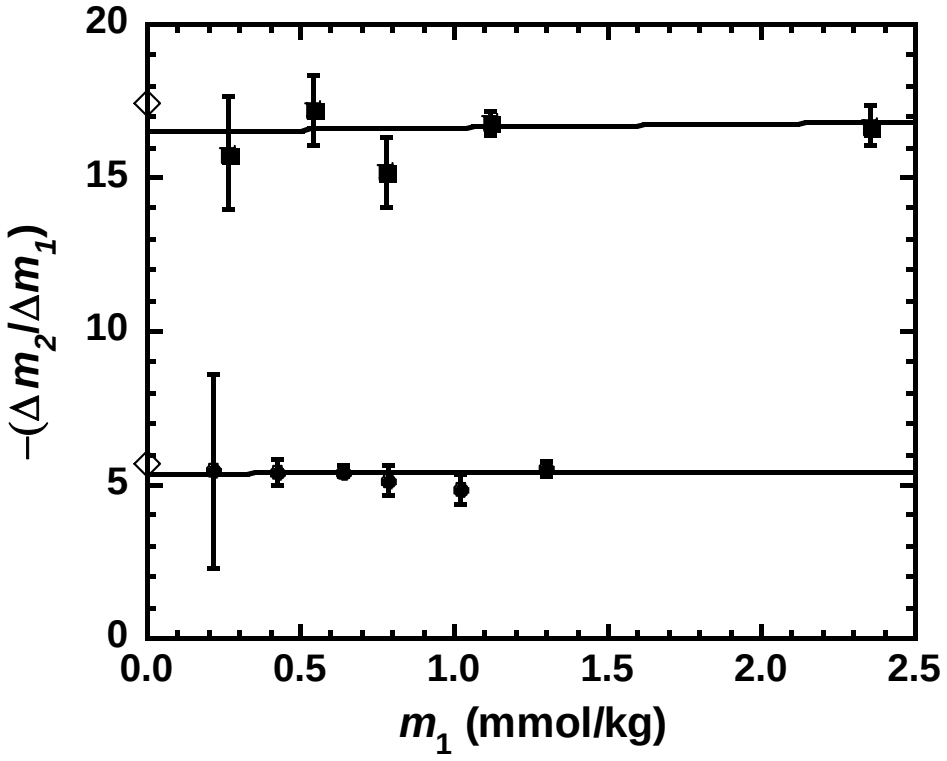

Figure 5. $-(\Delta m_2 / \Delta m_1)_{\mu_0=\mu_0'}$ as a function of m_1 at KCl 0.25 M (solid circles) and KCl 1.0 M (solid squares). The open diamonds represent the corresponding values of $-\Gamma_{12}$ obtained from diffusion measurements. The solid lines are weighed linear fits through the isopiestic data.

Chapter 6

Discussion and Conclusions

Introduction

In this chapter, we will first discuss my results on preferential-interaction coefficient and then examine the more complex behavior of the four diffusion coefficients. When appropriate, I will also compare my results on the PEG-KCl-water system with those previously obtained on the lysozyme-KCl-water at pH 4.5.

Preferential-interaction Coefficients

In Fig. 1, I plot $-\Gamma_{12}$ as a function of salt molality m_2 for both PEG (solid circles) and lysozyme (open circles) cases.

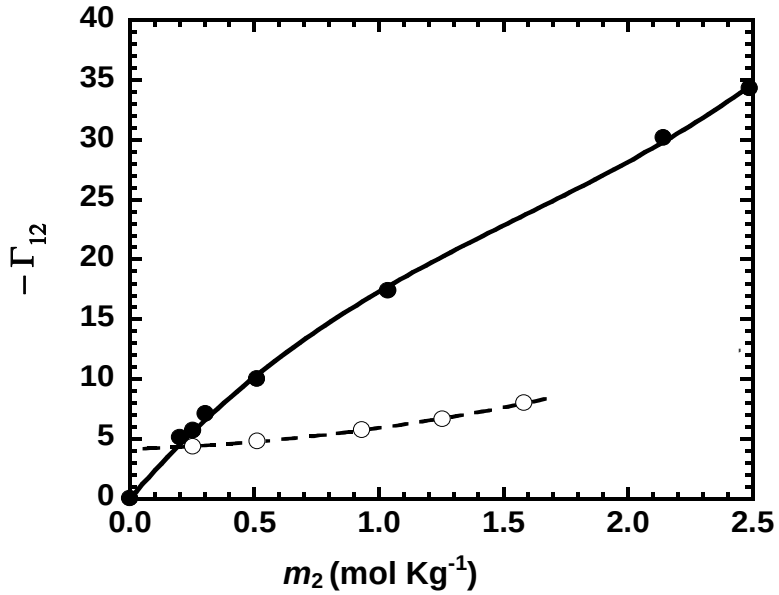

Figure 1. $-\Gamma_{12}$ as a function of m_2 for the PEG-KCl-H_2O system at 25 ºC (solid circles) and for the lysozyme-KCl-H_2O system at 25 ºC and pH 4.5 (open circles). The solid and dashed curves are fits through the data.

The first important difference between the PEG and lysozyme cases is at $m_2 = 0$. Since PEG is a neutral macromolecule, the condition $-\Gamma_{12}(0) = 0$ must be applied in this case, according to Eq. 16 of Chap. 2. On the other hand, since lysozyme is a charged macromolecule, we have: $-\Gamma_{12}(0) = z/2$, according to Eq. 33 of Chap. 2. For lysozyme, we fit the experimental data with a quadratic polynomial and determine: $z = 8 \pm 1$.[13] The z value corresponds to the protein cation's "effective charge" and is lower than the "net titration charge" This is expected, since the latter is based only on the degree of protonation and does not account for counterion binding. For lysozyme at pH 4.5, the net titration charge is 11.[85]

I now discuss the dependence of $-\Gamma_{12}$ on KCl concentration. For both macromolecular cases, $-\Gamma_{12}$ increases with m_2. This implies that both macromolecules are preferentially hydrated. In other words, we have macromolecule-salt net repulsive interactions in both cases. However, we observe the increase of $-\Gamma_{12}$ for the PEG case is significantly larger.

To better describe the difference in hydration between the two macromolecules, the two-domain model discussed in Chap. 2 can be used. Specifically, I use Eq. 12 of Chap. 2 to calculate the water excess $N_0(1-\alpha)$ for the PEG case. For the lysozyme case, $N_0(1-\alpha)$ can be calculate after removing the contribution of $z/2$ according to Eq. 33

of Chap. 2. In Fig. 2, I plot $N_0(1-\alpha)$ as a function of salt molality m_2 for both PEG (solid circles) and lysozyme (open circles) cases. We can see that the water excess for PEG is one order of magnitude larger than that of lysozyme, even though these two macromolecules have a similar molecular weight. Indeed the partial molar volume of lysozyme and PEG are $\bar{V}_1 = 10.2$ dm^3 mol^{-1} and $\bar{V}_1 = 16.8$ dm^{3}mol^{-1} respectively. The significant difference in water excess can be explained if we take into account the structural difference between a protein and polymer. Since a protein is a globular compact particle, only the particle surface is exposed to solvent. On the other hand, a polymer behaves like a coil where all monomers of the chain are exposed to the solvent. This is illustrated in Figs. 3.

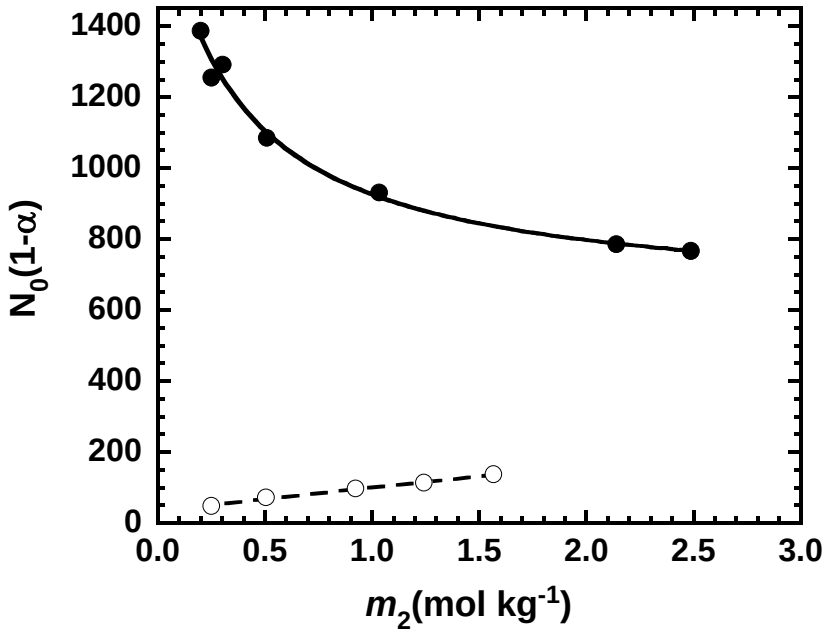

Figure 2. Water excess $N_0(1-\alpha)$ as a function of m_2 for the PEG-KCl-H_2O system at 25 ºC (solid circles) and for the lysozyme-KCl-H_2O system at 25 ºC and pH 4.5 (open circles). The solid and dashed curves are fits through the data.

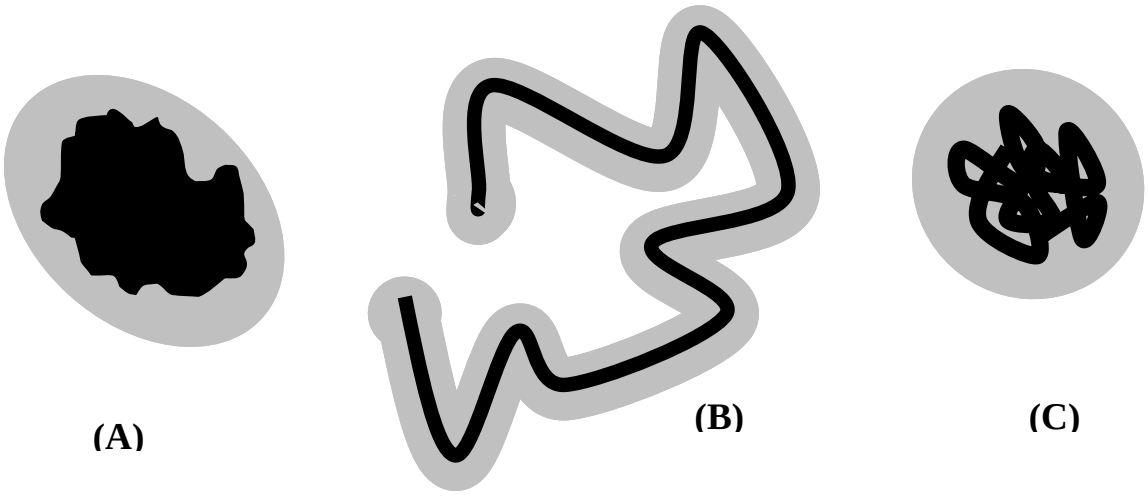

Figure 3. (A) Globular protein. (B) Expanded polymer. (C) Collapsed polymer. The gray areas represent the water excess. The water excess in (B) is larger than in (A) and

Furthermore, we observe that the water excess for PEG significantly decreases as salt concentration increases. This can be explained by observing that PEG will behave more like a compact globular particle as the salt concentration increases. In other words, the polymer collapses on itself due to PEG-KCl net repulsive interactions (see Fig. 3c).

Macromolecular hydration is expected to play an important role on the behavior of the four diffusion coefficients. In next section, I will discuss the diffusion behavior of PEG-KCl-water system.

Ternary Diffusion Coefficients

I will now examine our ternary diffusion coefficients. Since our values of D_{22} are closely related to the corresponding binary values, we will limit our discussion to the other three diffusion coefficients. I will specifically address the behavior of the solvent-frame $(D_{ij})_0$'s, due to their more direct connection to our thermodynamic results. Nevertheless, the difference between the values of $(D_{ij})_V$ and $(D_{ij})_0$ is small, and not relevant for the interpretations reported below. The main objective of this section is to understand how the behavior of the diffusion coefficients is related to preferential hydration.

Examination of D_{11}. Values of $(D_{11})_V$ for the PEG-KCl-water system are shown in Fig. 1 of Chap. 6. This diffusion coefficient D_{11} (i.e. $(D_{11})_V$ and $(D_{11})_0$) increases with salt concentration. Using Eq. 11a of Chap. 3, we can write:

$$\frac{(D_{11})_0}{RT} = (L_{11})_0 \hat{\mu}_{11}^{(c)} \left[1 + \frac{(L_{12})_0}{(L_{11})_0} \frac{\hat{\mu}_{21}^{(c)}}{\hat{\mu}_{11}^{(c)}} \right] \qquad (1)$$

For low concentration of neutral macromolecules, It is reasonable to assume that $(D_{11})_0 / RT = (L_{11})_0 \hat{\mu}_{11}^{(c)}$. $(L_{11})_0 \approx C_1 D_m$ and $\hat{\mu}_{11}^{(c)} \approx 1/C_1$, where D_m is the tracer diffusion coefficient of the macromolecule. According to the Stokes-Einstein equation

(Eq. 5 in Chap. 3), we can therefore write:

$$(D_{11})_0 \approx D_m = \frac{k_B T}{6\pi R_h \eta} \qquad (2)$$

Hence, according to Eq. 2, the D_{11} dependence on salt concentration can be attributed to changes in salt-water viscosity and macromolecule hydrodynamic radius, R_h. To remove the effect of viscosity, we consider the product: $(D_{11})_0(\eta/\eta_0)$ (see data in Table 1 of Chap. 5), where η is the viscosity of the corresponding binary salt-water systems and η_0 is the viscosity of water. In Fig. 4, I plot $(D_{11})_0(\eta/\eta_0)$ as a function of C_2. This plot shows that $(D_{11})_0(\eta/\eta_0)$ linearly increases with salt concentration. Note that $(D_{11})_0(\eta/\eta_0)$ decreases as the salt concentration increases in the case of lysozyme (data not shown).[13] According to Eq. 2, we can attribute the behavior shown in Fig. 4 to a decrease of the PEG hydrodynamic radius, R_h. This result is consistent with the observed decrease of water excess shown above in Fig. 2. In other words, the decrease of R_h can be attributed to the polymer collapse.

It is important to remember that PEG and salts have been employed together to induce phase transitions (e.g., crystallization and liquid-liquid phase separation) in proteins aqueous system. It is believed that the main action of PEG can be attributed to excluded-volume interactions between protein and PEG.[9, 35] One key parameter of these

interactions is the effective radius of the PEG molecules. Our results show that PEG radius decreases as salt concentration increase. Thus, salt can significantly affect protein-PEG interactions.

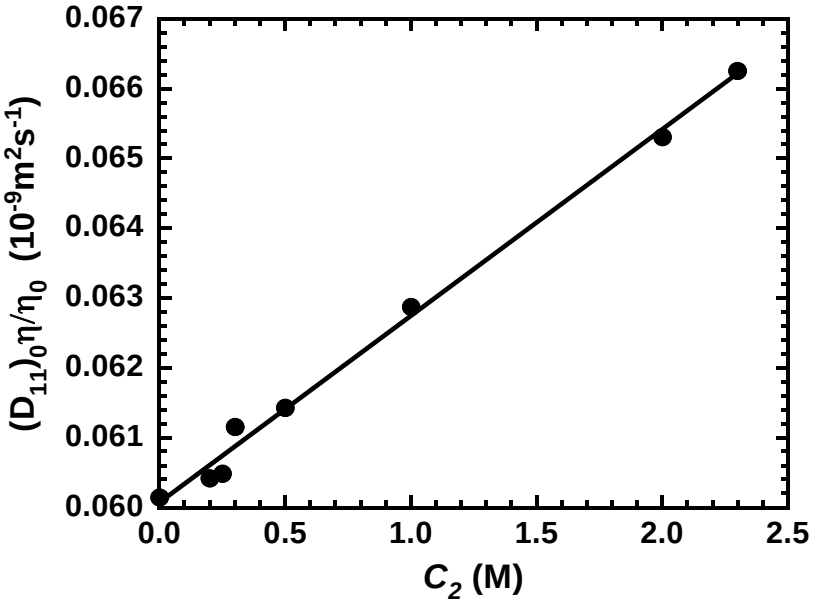

Figure 4. $(D_{11})_0(\eta/\eta_0)$ as a function of C_2 for the PEG-KCl-H_2O system at 25 ºC. The solid line is a linear fit through the data.

Examination of D_{12}. Values of $(D_{12})_V$ for the PEG-KCl-water system are shown in Fig. 2 of Chap. 6. This cross-diffusion coefficient describes how the flux of PEG is affected by the salt concentration gradient. Using Eq. 11b of Chap. 3, we can write:

$$\frac{(D_{12})_0}{RT} = (L_{11})_0 \hat{\mu}_{22}^{(c)} \left[\frac{\hat{\mu}_{12}^{(c)}}{\hat{\mu}_{22}^{(c)}} + \frac{(L_{12})_0}{(L_{11})_0} \right] \qquad (3)$$

For low concentration of neutral macromolecules, it is reasonable to assume that $(D_{12})_0 / RT = (L_{11})_0 \hat{\mu}_{22}^{(c)}$. $(L_{11})_0 \approx C_1 D_m$ and $\hat{\mu}_{12}^{(c)} / \hat{\mu}_{22}^{(c)} \approx \hat{\mu}_{12} / \hat{\mu}_{22} = -\Gamma_{12}$. Furthermore we can also consider the approximation: $\hat{\mu}_{22}^{(c)} \approx 2 / C_2$ since the thermodynamic deviation from ideality is not very large for KCl. Using these approximations, we can write:

$$\frac{(D_{12})_0}{C_1} \approx D_m \frac{(-\Gamma_{12})}{C_2} \approx D_m \frac{N_0(1-\alpha)}{m_0} \qquad (4)$$

Hence, according to Eq. 4, the ratio $(D_{12})_0 / C_1$ is approximately directly proportional to the water excess. Using Eq. 4 with $D_m \approx 0.06\ 10^{-9}$ $m^2 s^{-1}$ and the values of $(D_{12})_0$ in Table 1 of Chap. 5, we estimate: $N_0(1-\alpha) \approx 300$, which is in qualitative agreement with the values shown in Fig. 2. In Fig. 5, we show $(D_{12})_0 / C_1$ for both the PEG and the lysozyme case.

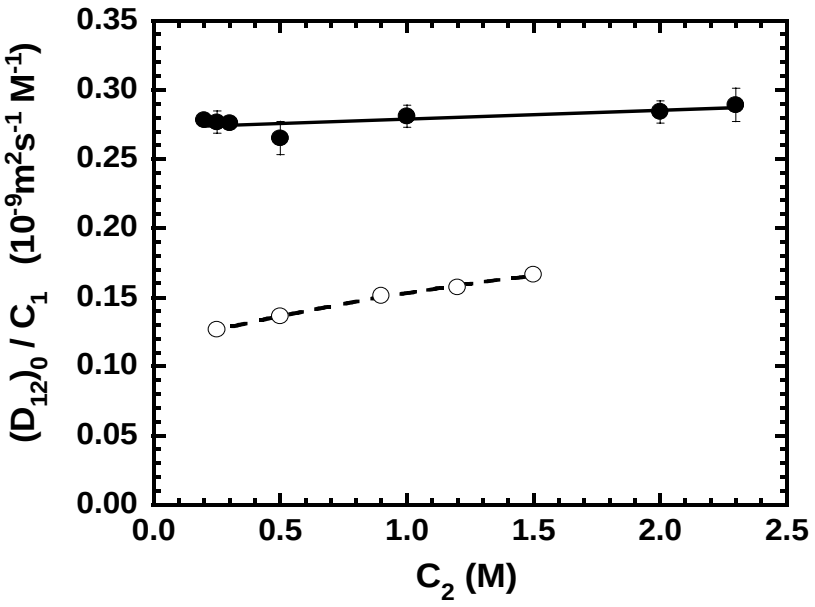

Figure 5. $(D_{12})_0 / C_1$ as a function of C_2 for the PEG-KCl-H_2O system at 25 ºC (solid circles) and for the lysozyme-KCl-H_2O system at 25 ºC and pH 4.5 (open circles). The solid and dashed curves are fits through the data.

It is important to note that $D_m \approx 0.12\ 10^{-9}$ $m^2 s^{-1}$ for lysozyme.[13] This value is about two times higher than that of PEG.. Nonetheless, in Fig. 5, we observe that the $(D_{12})_0 / C_1$ values for lysozyme are only about half the value obtained for PEG. We therefore conclude that the $(D_{12})_0 /(C_1 D_m)$ values for PEG are about four times the values shown for lysozyme. This result is in qualitative agreement with the observed difference in water excess between PEG and lysozyme.

Examination of D_{21}. Values of $(D_{21})_V$ for the PEG-KCl-water system are shown in Fig. 3 of Chap. 6. This cross-diffusion coefficient describes how the flux of salt is affected by the PEG concentration gradient. Using Eqs. 10,11c of Chap. 3, we can write:

$$\frac{(D_{21})_0}{RT} = (L_{22})_0 \hat{\mu}_{22}^{(c)} \left[\frac{\hat{\mu}_{21}^{(c)}}{\hat{\mu}_{22}^{(c)}} + \frac{(L_{12})_0}{(L_{22})_0} \frac{\hat{\mu}_{11}^{(c)}}{\hat{\mu}_{22}^{(c)}} \right] \tag{5}$$

For low concentration of neutral macromolecules, it is reasonable to assume that $(D_{21})_0 / RT \approx (L_{22})_0 \hat{\mu}_{21}^{(c)}$ and $(D_{22})_0 / RT \approx (L_{22})_0 \hat{\mu}_{22}^{(c)}$. Hence, according to Eq. 5, we can write the following approximate equation:

$$\frac{(D_{21})_0}{(D_{22})_0} \approx \frac{\hat{\mu}_{21}^{(c)}}{\hat{\mu}_{22}^{(c)}} \tag{6}$$

According to Eqs. 12(a-d) of Chap. 3, we can approximately write:

$$\hat{\mu}_{21}^{(c)} \approx \hat{\mu}_{12}^{(c)} + C_2 \overline{V}_1 \hat{\mu}_{22}^{(c)} \tag{7}$$

where we have used $\hat{\mu}_{12}^{(c)} \approx \hat{\mu}_{12}$ and $\hat{\mu}_{22}^{(c)} \approx \hat{\mu}_{22}$. We can combine Eq. 6 and Eq. 7 with the definition of Γ_{12} and write:

$$\frac{(D_{21})_0}{(D_{22})_0} \approx (-\Gamma_{12}) + C_2 \overline{V}_1 \tag{8}$$

In Fig. 6, I show the $(D_{21})_0/(D_{22})_0$ values for the PEG and lysozyme cases as a function of C_2. The corresponding curves increase with salt concentrations and display a behavior similar to that shown in Fig. 1 for $-\Gamma_{12}$. This is consistent with Eq. 8. Furthermore the values of $(D_{21})_0/(D_{22})_0$ are systematically higher than the corresponding values of $-\Gamma_{12}$ due to the positive contribution of $C_2\bar{V}_1$.

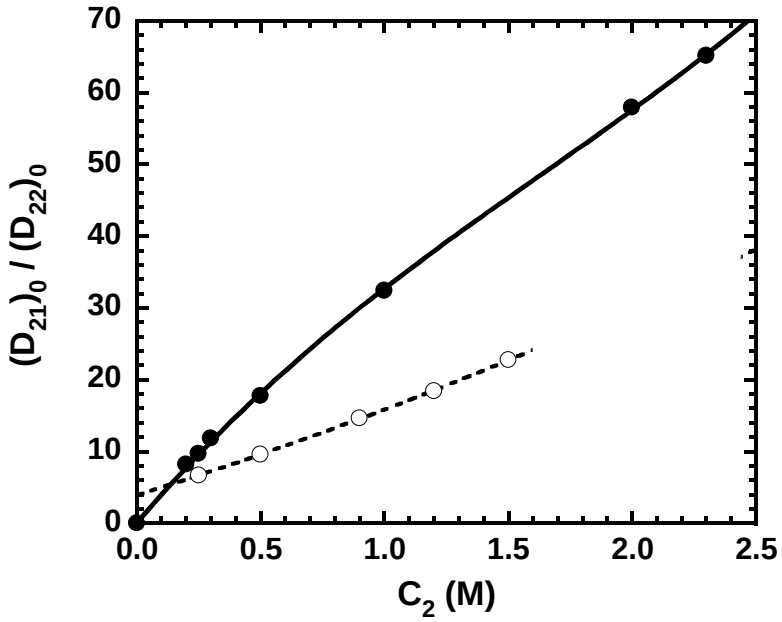

Figure 6. $(D_{21})_0/(D_{22})_0$ as a function of C_2 for the PEG-KCl-H_2O system at 25 ºC (solid circles) and for the lysozyme-KCl-H_2O system at 25 ºC and pH 4.5 (open circles). The solid and dashed curves are fits through the data.

Conclusions

The central goal of this thesis is to show how multicomponent diffusion of polymer-salt-solvent systems is directly related polymer-salt thermodynamic interactions.

First, the experimental comparison between diffusion and isopiestic measurements has allowed us to demonstrate that ternary diffusion coefficients can be indeed be used to determine preferential-interaction coefficients. From this perspective, my experimental work has been important not only for the examination of the accuracy of the thermodynamic data obtained using multicomponent diffusion but has also provided a significant contribution to the validation of three postulates of non-equilibrium thermodynamics applied to the diffusion processes.

Second, we have observed a marked difference between protein hydration and PEG hydration. We can attribute this difference to the corresponding structural difference between a polymer and a protein. Furthermore, by examining the two cross-diffusion coefficients, we can conclude that their magnitude increase with the magnitude of preferential hydration.

Understanding and tuning the magnitude of cross-diffusion coefficients is important for accurate modeling of mass-transfer processes, especially those occurring in the presence of large solute gradients. Indeed cross-diffusion coefficients could be generally used to control the diffusion rate of target solutes. For example, the diffusion rate of a given drug from a delivery porous device (e.g. gels) may be controlled by the concentration gradient of an additive embedded in the same device. Since PEG hydration brings about large cross-diffusion coefficients, concentration gradients of this slow macromolecule could be

used to tune the diffusion rate of small drug molecules. Examples of diffusion-based applications in the presence of large solute gradients is the free-interface diffusion obtained in microfluidic devices, gels and microgravity. Here, the effect of spatial and temporal changes of a chemical environment on a target solute are investigated by interfacing a solution containing the target solute with one containing an additive. For microfluidic devices, the free-interface diffusion shown in Fig. 7 is also at the heart of the intermixing between two or more laminar fluid streams. For several microfluidic processes, a correct contact length (*l* in Fig. 5) between two fluids (together with the flow rate) must be chosen depending on whether fast complete mixing (relevant to reaction kinetics) or only slow partial mixing (relevant to diffusion-based separation of two molecules or crystallization) is needed. Clearly, multicomponent diffusion coefficients are valuable for designing these processes. Hence my thesis will stimulate more diffusion investigations on PEG ternary systems.

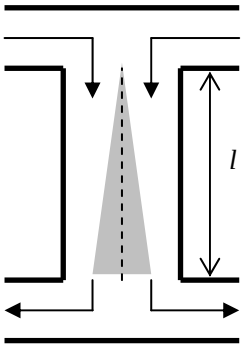

Figure 7. Mixing between two laminar fluids based on diffusion. The gray area is the interdiffusion zone.

Appendix

Diffusion Experiments

In Tables A1-7, data relative to solutions preparation and diffusion coefficients results are listed. For each ternary point four experiments are reported (A, B, C, D): two at $\alpha \approx 0$ and two at $\alpha \approx 1$.

In these tables, the following values are reported:

1) $\overline{C_i}$,component *i* average molar concentration for the bottom-top pair solutions;

2) ΔC_i , component *i* molar concentration difference between bottom and top solutions;

3) $d_{\text{bot/top}}$, density for bottom and top solutions;

4) J_{meas}, total number of fringes measured in the particular experiment;

5) J_{calc}, total number of fringes determined by $J = R_1\Delta C_1 + R_2\Delta C_2$;

6) D_A, pseudo-binary diffusion coefficient calculated by $\frac{1}{\sqrt{D_A}} = \sum_i \Gamma_i \frac{1}{\sqrt{\lambda_i}}$;

7) $\overline{\overline{C_i}}$,component *i* average molar concentration determined from the complete set of experiments;

8) $\overline{d}$, H_i fitting parameters determined from $d = \overline{d} + H_1\left(C_1 - \overline{\overline{C_1}}\right) + H_2\left(C_2 - \overline{\overline{C_2}}\right)$;

9) $\overline{V_i}$, component *i* partial molar volume;

10) R_i , component *i* instrumental refractive index derivative $\frac{l}{\lambda}\frac{\partial n}{\partial c_i}$;

11) Λ_i , i^{th} eigenvalue of the matrix of volume-fixed diffusion;

12) $\left(D_{ij}\right)_V$, volume-frame diffusion coefficients;

13) $\left(D_{ij}\right)_0$, solvent-frame diffusion coefficients.

Ternary Diffusion Experiments for PEG-KCl-Water system at T=25 ºC

Ternary table A1

expt pkc1	A $\alpha = 0$ Pkc1e	B $\alpha = 0$ pkc1j	C $\alpha = 1$ pkc1g	D $\alpha = 1$ pkc1h
$\overline{C}_1$ (mmol dm^{-3})	0.2500	0.2500	0.2500	0.2500
$\overline{C}_2$ (mol dm^{-3})	0.9999	0.9999	0.9999	0.9996
ΔC_1 (mmol dm^{-3})	0.0000	0.0000	0.4990	0.4990
ΔC_2 (mol dm^{-3})	0.1284	0.1284	-0.0151	-0.0144
d (g cm^{-3}) bot	1.040747	1.040756	1.043172	1.042834
d (g cm^{-3}) top	1.046499	1.046486	1.044095	1.044085
J meas	54.8314	54.8568	54.7495	58.0353
J calc	54.8361	54.8511	54.7329	58.0519
D_A (10^{-9} m^2 s^{-1})	2.00171	2.00130	0.06189	0.06816

$\overline{\overline{C}}_1$ (mmol dm^{-3})	0.2500		
$\overline{\overline{C}}_2$ (mol dm^{-3})	0.9998	Λ_1 (10^{-9} m^2 s^{-1})	0.06042
		Λ_2 (10^{-9} m^2 s^{-1})	1.861
$\overline{d}$ (g cm^{-3})	1.043622		
H_1 (dm^3 mol^{-1})	3.193	$(D_{11})_V$ (10^{-9} m^2 s^{-1})	0.06230±0.00010
H_2 (dm^3 mol^{-1})	0.04471	$(D_{12})_V$ (10^{-9} m^2 s^{-1})	0.000056±0.000002
		$(D_{21})_V$ (10^{-9} m^2 s^{-1})	61.0±0.2
$\overline{V}_0$ (dm^3 mol^{-1})	0.01805	$(D_{22})_V$ (10^{-9} m^2 s^{-1})	1.859±0.001
$\overline{V}_1$ (dm^3 mol^{-1})	16.84		
$\overline{V}_2$ (dm^3 mol^{-1})	0.02991	$(D_{11})_0$ (10^{-9} m^2 s^{-1})	0.06304
		$(D_{12})_0$ (10^{-9} m^2 s^{-1})	0.000070
R_1 (dm^3 mol^{-1})	122584	$(D_{21})_0$ (10^{-9} m^2 s^{-1})	64.0
R_2 (dm^3 mol^{-1})	427.1	$(D_{22})_0$ (10^{-9} m^2 s^{-1})	1.919

Ternary table A2

expt pkc2	A $\alpha = 0$ Pkc2a'	B $\alpha = 0$ Pkc2d	C $\alpha = 1$ Pkc2b	D $\alpha = 1$ Pkc2c
$\overline{C}_1$ (mmol dm^{-3})	0.2500	0.2500	0.2500	0.2500
$\overline{C}_2$ (mol dm^{-3})	0.5000	0.5000	0.5000	0.5000
ΔC_1 (mmol dm^{-3})	0.0000	0.0000	0.4695	0.4695
ΔC_2 (mol dm^{-3})	0.1239	0.1239	-0.0062	-0.0062
d (g cm^{-3}) bot	1.018227	1.018225	1.020436	1.020436
d (g cm^{-3}) top	1.023897	1.023898	1.021680	1.021676
J meas	54.8920	54.8980	55.1150	55.1380
J calc	54.8930	54.8970	55.1171	55.1359
D_A (10^{-9} m^2 s^{-1})	1.95141	1.95141	0.06206	0.06208

$\overline{\overline{C}}_1$ (mmol dm^{-3})	0.2500		
$\overline{\overline{C}}_2$ (mol dm^{-3})	0.5000	Λ_1 (10^{-9} m^2 s^{-1})	0.06010
		Λ_2 (10^{-9} m^2 s^{-1})	1.817
$\overline{d}$ (g cm^{-3})	1.021060		
H_1 (dm^3 mol^{-1})	3.250	$(D_{11})_V$ (10^{-9} m^2 s^{-1})	0.06107 ±0.00012
H_2 (dm^3 mol^{-1})	0.04578	$(D_{12})_V$ (10^{-9} m^2 s^{-1})	0.000053±0.000003
		$(D_{21})_V$ (10^{-9} m^2 s^{-1})	32.2±0.3
$\overline{V}_0$ (dm^3 mol^{-1})	0.01806	$(D_{22})_V$ (10^{-9} m^2 s^{-1})	1.816±0.002
$\overline{V}_1$ (dm^3 mol^{-1})	16.79		
$\overline{V}_2$ (dm^3 mol^{-1})	0.02885	$(D_{11})_0$ (10^{-9} m^2 s^{-1})	0.06160
		$(D_{12})_0$ (10^{-9} m^2 s^{-1})	0.000066
R_1 (dm^3 mol^{-1})	123266	$(D_{21})_0$ (10^{-9} m^2 s^{-1})	33.2
R_2 (dm^3 mol^{-1})	443.1	$(D_{22})_0$ (10^{-9} m^2 s^{-1})	1.843

Ternary table A3

expt pkc3	A $\alpha = 0$ pkc3a	B $\alpha = 0$ pkc3e	C $\alpha = 1$ pkc3b	D $\alpha = 1$ pkc3g
$\overline{C_1}$ (mmol dm^{-3})	0.2500	0.2500	0.2500	0.2500
$\overline{C_2}$ (mol dm^{-3})	2.0001	2.0000	2.0001	1.9998
ΔC_1 (mmol dm^{-3})	0.0000	0.0000	0.4878	0.4877
ΔC_2 (mol dm^{-3})	0.1337	0.1336	-0.0247	-0.0244
d (g cm^{-3}) bot	1.084628	1.084649	1.087311	1.087285
d (g cm^{-3}) top	1.090409	1.090424	1.087727	1.087747
J meas	53.8066	53.8600	49.3957	49.2828
J calc	53.8507	53.8157	49.2947	49.3839
D_A (10^{-9} m^2 s^{-1})	2.09839	2.09872	0.06525	0.06545

$\overline{\overline{C_1}}$ (mmol dm^{-3})	0.2500		
$\overline{\overline{C_2}}$ (mol dm^{-3})	2.0000	Λ_1 (10^{-9} m^2 s^{-1})	0.06016
		Λ_2 (10^{-9} m^2 s^{-1})	1.967
$\overline{d}$ (g cm^{-3})	1.087522		
H_1 (dm^3 mol^{-1})	3.074	$(D_{11})_V$ (10^{-9} m^2 s^{-1})	0.06356±0.00016
H_2 (dm^3 mol^{-1})	0.04324	$(D_{12})_V$ (10^{-9} m^2 s^{-1})	0.000054±0.000002
		$(D_{21})_V$ (10^{-9} m^2 s^{-1})	119.0±0.9
$\overline{V_0}$ (dm^3 mol^{-1})	0.01801	$(D_{22})_V$ (10^{-9} m^2 s^{-1})	1.963±0.002
$\overline{V_1}$ (dm^3 mol^{-1})	16.92		
$\overline{V_2}$ (dm^3 mol^{-1})	0.03131	$(D_{11})_0$ (10^{-9} m^2 s^{-1})	0.06489
		$(D_{12})_0$ (10^{-9} m^2 s^{-1})	0.000071
R_1 (dm^3 mol^{-1})	121421	$(D_{21})_0$ (10^{-9} m^2 s^{-1})	129.3
R_2 (dm^3 mol^{-1})	402.9	$(D_{22})_0$ (10^{-9} m^2 s^{-1})	2.097

Ternary table A4

expt Pkc4	A $\alpha = 0$ Pkc4a	B $\alpha = 0$ Pkc4d	C $\alpha = 1$ Pkc4b	D $\alpha = 1$ Pkc4c
$\overline{C_1}$ (mmol dm^{-3})	0.2500	0.2500	0.2500	0.2500
$\overline{C_2}$ (mol dm^{-3})	0.2500	0.2500	0.2500	0.2500
ΔC_1 (mmol dm^{-3})	0.0000	0.0000	0.4561	0.4561
ΔC_2 (mol dm^{-3})	0.1212	0.1212	-0.0024	-0.0024
d (g cm^{-3}) bot	1.006747	1.006734	1.008868	1.008859
d (g cm^{-3}) top	1.012360	1.012364	1.010247	1.010248
J meas	54.9192	54.8400	55.2154	55.2034
J calc	54.8764	54.8828	55.2092	55.2096
D_A (10^{-9} m^2 s^{-1})	1.95506	1.95385	0.06134	0.06134

$\overline{\overline{C_1}}$ (mmol dm^{-3})	0.2500		
$\overline{\overline{C_2}}$ (mol dm^{-3})	0.2500	Λ_1 (10^{-9} m^2 s^{-1})	0.05960
		Λ_2 (10^{-9} m^2 s^{-1})	1.809
$\overline{d}$ (g cm^{-3})	1.009553		
H_1 (dm^3 mol^{-1})	3.282	$(D_{11})_V$ (10^{-9} m^2 s^{-1})	0.06016±0.00007
H_2 (dm^3 mol^{-1})	0.04640	$(D_{12})_V$ (10^{-9} m^2 s^{-1})	0.000056±0.000002
		$(D_{21})_V$ (10^{-9} m^2 s^{-1})	17.4±0.2
$\overline{V_0}$ (dm^3 mol^{-1})	0.01807	$(D_{22})_V$ (10^{-9} m^2 s^{-1})	1.809±0.002
$\overline{V_1}$ (dm^3 mol^{-1})	16.77		
$\overline{V_2}$ (dm^3 mol^{-1})	0.02824	$(D_{11})_0$ (10^{-9} m^2 s^{-1})	0.06048
		$(D_{12})_0$ (10^{-9} m^2 s^{-1})	0.000069
R_1 (dm^3 mol^{-1})	123465	$(D_{21})_0$ (10^{-9} m^2 s^{-1})	17.8
R_2 (dm^3 mol^{-1})	452.9	$(D_{22})_0$ (10^{-9} m^2 s^{-1})	1.822

Ternary table A5

expt pkc5	A $\alpha = 0$ Pkc5a	B $\alpha = 0$ Pkc5d	C $\alpha = 1$ Pkc5b	D $\alpha = 1$ Pkc5c
$\overline{C}_1$ (mmol dm^{-3})	0.2500	0.2500	0.2500	0.2500
$\overline{C}_2$ (mol dm^{-3})	0.3000	0.3000	0.3000	0.3000
ΔC_1 (mmol dm^{-3})	0.0000	0.0000	0.4605	0.4605
ΔC_2 (mol dm^{-3})	0.1217	0.1217	-0.0037	-0.0037
d (g cm^{-3}) bot	1.009053	1.009057	1.011202	1.011197
d (g cm^{-3}) top	1.014684	1.014691	1.012542	1.012549
J meas	54.8360	54.8607	55.2796	55.1807
J calc	54.8477	54.8490	55.2317	55.2286
D_A (10^{-9} m^2 s^{-1})	1.94864	1.94833	0.06171	0.06171

$\overline{\overline{C}}_1$ (mmol dm^{-3})	0.2500		
$\overline{\overline{C}}_2$ (mol dm^{-3})	0.3000	Λ_1 (10^{-9} m^2 s^{-1})	0.06014
		Λ_2 (10^{-9} m^2 s^{-1})	1.805
$\overline{d}$ (g cm^{-3})	1.011872		
H_1 (dm^3 mol^{-1})	3.292	$(D_{11})_V$ (10^{-9} m^2 s^{-1})	0.06082±0.00003
H_2 (dm^3 mol^{-1})	0.04628	$(D_{12})_V$ (10^{-9} m^2 s^{-1})	0.000056±0.000001
		$(D_{21})_V$ (10^{-9} m^2 s^{-1})	21.2±0.1
$\overline{V}_0$ (dm^3 mol^{-1})	0.01807	$(D_{22})_V$ (10^{-9} m^2 s^{-1})	1.804±0.005
$\overline{V}_1$ (dm^3 mol^{-1})	16.76		
$\overline{V}_2$ (dm^3 mol^{-1})	0.02836	$(D_{11})_0$ (10^{-9} m^2 s^{-1})	0.06121
		$(D_{12})_0$ (10^{-9} m^2 s^{-1})	0.000069
R_1 (dm^3 mol^{-1})	123532	$(D_{21})_0$ (10^{-9} m^2 s^{-1})	21.6
R_2 (dm^3 mol^{-1})	450.8	$(D_{22})_0$ (10^{-9} m^2 s^{-1})	1.820

Ternary table A6

expt pkc6	A $\alpha = 0$ Pkc6a	B $\alpha = 0$ Pkc6d	C $\alpha = 1$ Pkc6b	D $\alpha = 1$ Pkc6c
$\overline{C}_1$ (mmol dm^{-3})	0.2500	0.2500	0.2500	0.2500
$\overline{C}_2$ (mol dm^{-3})	0.2000	0.2000	0.2000	0.2000
ΔC_1 (mmol dm^{-3})	0.0000	0.0000	0.3736	0.3736
ΔC_2 (mol dm^{-3})	0.1000	0.0999	-0.0010	-0.0010
d (g cm^{-3}) bot	1.004922	1.004926	1.006657	1.006659
d (g cm^{-3}) top	1.009560	1.009576	1.007840	1.007838
J meas	45.5705	45.5285	45.7060	45.6708
J calc	45.5572	45.5418	45.6885	45.6883
D_A (10^{-9} m^2 s^{-1})	1.95167	1.95162	0.061681	0.06181

$\overline{\overline{C}}_1$ (mmol dm^{-3})	0.2500		
$\overline{\overline{C}}_2$ (mol dm^{-3})	0.2000	Λ_1 (10^{-9} m^2 s^{-1})	0.05962
		Λ_2 (10^{-9} m^2 s^{-1})	1.805
$\overline{d}$ (g cm^{-3})	1.007247		
H_1 (dm^3 mol^{-1})	3.284	$(D_{11})_V$ (10^{-9} m^2 s^{-1})	0.06010± 0.00004
H_2 (dm^3 mol^{-1})	0.04646	$(D_{12})_V$ (10^{-9} m^2 s^{-1})	0.000056±0.000001
		$(D_{21})_V$ (10^{-9} m^2 s^{-1})	14.7±0.1
$\overline{V}_0$ (dm^3 mol^{-1})	0.01807	$(D_{22})_V$ (10^{-9} m^2 s^{-1})	1.804±0.001
$\overline{V}_1$ (dm^3 mol^{-1})	16.76		
$\overline{V}_2$ (dm^3 mol^{-1})	0.02819	$(D_{11})_0$ (10^{-9} m^2 s^{-1})	0.06046
		$(D_{12})_0$ (10^{-9} m^2 s^{-1})	0.000070
R_1 (dm^3 mol^{-1})	123484	$(D_{21})_0$ (10^{-9} m^2 s^{-1})	15.0
R_2 (dm^3 mol^{-1})	455.7	$(D_{22})_0$ (10^{-9} m^2 s^{-1})	1.814

Ternary table A7

expt pkc7	A $\alpha = 0$ Pkc7a	B $\alpha = 0$ Pkc7d	C $\alpha = 1$ Pkc7b	D $\alpha = 1$ Pkc7c
$\overline{C}_1$ (mmol dm^{-3})	0.2500	0.2500	0.2500	0.2499
$\overline{C}_2$ (mol dm^{-3})	2.2996	2.2996	2.2998	2.2996
ΔC_1 (mmol dm^{-3})	0.0000	0.0000	0.4499	0.4499
ΔC_2 (mol dm^{-3})	0.1379	0.1382	-0.0263	-0.0266
d (g cm^{-3}) bot	1.097471	1.097424	1.100312	1.100296
d (g cm^{-3}) top	1.103365	1.103368	1.100570	1.100504
J meas	54.3533	54.6012	43.9986	43.9075
J calc	54.4146	54.5401	44.0166	43.8895
D_A (10^{-9} m^2 s^{-1})	2.13515	2.13403	0.065555	0.06526

$\overline{\overline{C}}_1$ (mmol dm^{-3})	0.2500		
$\overline{\overline{C}}_2$ (mol dm^{-3})	2.2996	Λ_1 (10^{-9} m^2 s^{-1})	0.06002
		Λ_2 (10^{-9} m^2 s^{-1})	2.001
$\overline{d}$ (g cm^{-3})	1.100414		
H_1 (dm^3 mol^{-1})	3.036	$(D_{11})_V$ (10^{-9} m^2 s^{-1})	0.06393±0.00020
H_2 (dm^3 mol^{-1})	0.04289	$(D_{12})_V$ (10^{-9} m^2 s^{-1})	0.000055±0.000003
		$(D_{21})_V$ (10^{-9} m^2 s^{-1})	137.9±0.6
$\overline{V}_0$ (dm^3 mol^{-1})	0.01800	$(D_{22})_V$ (10^{-9} m^2 s^{-1})	1.997±0.002
$\overline{V}_1$ (dm^3 mol^{-1})	16.95		
$\overline{V}_2$ (dm^3 mol^{-1})	0.03164	$(D_{11})_0$ (10^{-9} m^2 s^{-1})	0.06537
		$(D_{12})_0$ (10^{-9} m^2 s^{-1})	0.000072
R_1 (dm^3 mol^{-1})	120875	$(D_{21})_0$ (10^{-9} m^2 s^{-1})	151.5
R_2 (dm^3 mol^{-1})	102.1	$(D_{22})_0$ (10^{-9} m^2 s^{-1})	2.162

Binary Diffusion Experiments for KCl-Water system at T=25 ºC

In Table A8, I report the diffusion data for the corresponding binary salt-water solutions.

Table A8

	bk1	bk2	bk3	bk4	bk5	bk6	bk7
$\overline{C}_2$ (mol dm^{-3})	0.9998	0.4999	2.0002	0.2500	0.3000	0.2000	2.2999
ΔC_2 (mol dm^{-3})	0.1285	0.1241	0.1336	0.1211	0.1211	0.1000	0.1380
d (g cm^{-3}) bot	1.045697	1.023073	1.089645	1.011555	1.013858	1.008742	1.102617
d (g cm^{-3}) top	1.039956	1.017387	1.083887	1.005948	1.008255	1.004103	1.096681
J meas	54.9810	55.1320	53.7580	55.0200	54.6540	45.6020	54.553
R_2 (dm^3 mol^{-1})	427.7	444.3	402.4	454.2	451.2	456.1	395.28
D_2 (10^{-9} m^2 s^{-1})	1.8924	1.8480	1.9938	1.8388	1.8379	1.8352	2.0321
$\overline{d}$ (g cm^{-3})	1.041744	1.019934	1.083529	1.008644	1.010930	1.006336	1.095691
H_2 (kg mol^{-1})	0.04471	0.04578	0.04324	0.04640	0.04628	0.04646	0.04289
$\overline{V}_0$ (dm^3 mol^{-1})	0.01760	0.01788	0.01700	0.01802	0.01799	0.01804	0.01682
$\overline{V}_2$ (dm^3 mol^{-1})	0.02994	0.02886	0.03142	0.02825	0.02836	0.02819	0.03176

Isopiestic Experiments

In Tables A9-14, I report the six isopiestic experiments corresponding to the average salt molality $\approx 0.25\,\mathrm{mol\,kg^{-1}}$, and in Tables A15-19, I report the five isopiestic experiments corresponding to the average salt molality $\approx 1\,\mathrm{mol\,kg^{-1}}$.

In these tables, the following values are reported:

1) m_1, m_2 are the molalities of PEG and KCl respectively for the ternary PEG-KCl-water system;
2) m_2' is the molality of KCl for the binary KCl-water system;
3) $\overline{m}_1$, $\overline{m}_2$ and $\overline{m}_2'$ are the average molalities;
4) σ_{m_1} , σ_{m_2} and $\sigma_{m_2'}$ are the relative standard errors;
5) $\Delta m_2 / \Delta m_1 = (\overline{m}_2 - \overline{m}_2') / \overline{m}_1$;
6) $\sigma_{\Delta m_2 / \Delta m_1}$ is the relative standard error of the $(m_2 - m_2') / m_1$ values.

Table A9

m_1 (mmol Kg^{-1})	m_2 (mol Kg^{-1})	m_2' (mol Kg^{-1})	$\overline{m}_1$ (mmol Kg^{-1})	0.7861
0.7870	0.2619	0.2656	σ_{m_1} (mmol Kg^{-1})	0.0011
0.7853	0.2613	0.2657	$\overline{m}_2$ (mol Kg^{-1})	0.2616
			σ_{m_2} (mol Kg^{-1})	0.0004
			$\overline{m}_2'$ (mol Kg^{-1})	0.2656
			$\sigma_{m_2'}$ (mol Kg^{-1})	0.0001
			$\Delta m_2 / \Delta m_1$	-5.1444
			$\sigma_{\Delta m_2 / \Delta m_1}$	-0.4899

Table A10

m_1 (mmol Kg^{-1})	m_2 (mol Kg^{-1})	m_2' (mol Kg^{-1})	$\overline{m}_1$ (mmol Kg^{-1})	1.0242
1.0239	0.2564	0.2611	σ_{m_1} (mmol Kg^{-1})	0.0005
1.0248	0.2566	0.2609	$\overline{m}_2$ (mol Kg^{-1})	0.2564
1.0246	0.2565	0.2618	σ_{m_2} (mol Kg^{-1})	0.0001
1.0237	0.2563	0.2618	$\overline{m}_2'$ (mol Kg^{-1})	0.2614
			$\sigma_{m_2'}$ (mol Kg^{-1})	0.0005
			$\Delta m_2 / \Delta m_1$	-4.8467
			$\sigma_{\Delta m_2 / \Delta m_1}$	0.4660

Table A11

m_1 (mmol Kg^{-1})	m_2 (mol Kg^{-1})	m_2' (mol Kg^{-1})	$\overline{m}_1$ (mmol Kg^{-1})	1.2970
1.2980	0.2601	0.2670	σ_{m_1} (mmol Kg^{-1})	0.0011
0.1296	0.2596	0.2674	$\overline{m}_2$ (mol Kg^{-1})	0.2599
1.2972	0.2599	0.2669	σ_{m_2} (mol Kg^{-1})	0.0002
			$\overline{m}_2'$ (mol Kg^{-1})	0.2671
			$\sigma_{m_2'}$ (mol Kg^{-1})	0.0003
			$\Delta m_2 / \Delta m_1$	-5.5416
			$\sigma_{\Delta m_2 / \Delta m_1}$	0.2625

Table A12

m_1 (mmol Kg^{-1})	m_2 (mol Kg^{-1})	m_2' (mol Kg^{-1})	$\overline{m}_1$(mmol Kg^{-1})	0.2131
0.2125	0.2657	0.2676	σ_{m_1} (mmol Kg^{-1})	0.0005
0.2129	0.2662	0.2671	$\overline{m}_2$(mol Kg^{-1})	0.2664
0.2133	0.2667	0.2671	σ_{m_2} (mol Kg^{-1})	0.0006
0.2137	0.2671	0.2684	$\overline{m}_2'$(mol Kg^{-1})	0.2676
			$\sigma_{m_2'}$ (mol Kg^{-1})	0.0006
			$\Delta m_2 / \Delta m_1$	-5.4696
			$\sigma_{\Delta m_2 / \Delta m_1}$	3.1473

Table A13

m_1 (mmol Kg^{-1})	m_2(mol Kg^{-1})	m_2' (mol Kg^{-1})	$\overline{m}_1$(mmol Kg^{-1})	0.4233
0.4232	0.2644	0.2667	σ_{m_1} (mmol Kg^{-1})	0.0002
0.4231	0.2643	0.2666	$\overline{m}_2$(mol Kg^{-1})	0.2644
0.4236	0.2646	0.2668	σ_{m_2} (mol Kg^{-1})	0.0001
0.4232	0.2644	0.2669	$\overline{m}_2'$(mol Kg^{-1})	0.2668
			$\sigma_{m_2'}$ (mol Kg^{-1})	0.0001
			$\Delta m_2 / \Delta m_1$	-5.4530
			$\sigma_{\Delta m_2 / \Delta m_1}$	0.4203

Table A14

m_1 (mmol Kg^{-1})	m_2(mol Kg^{-1})	m_2' (mol Kg^{-1})	$\overline{m}_1$(mmol Kg^{-1})	0.6370
0.6370	0.2649	0.2683	σ_{m_1} (mmol Kg^{-1})	0.0001
0.6370	0.2649	0.2683	$\overline{m}_2$(mol Kg^{-1})	0.2649
0.6371	0.2650	0.2685	σ_{m_2} (mol Kg^{-1})	0.0000
0.6369	0.2649	0.2685	$\overline{m}_2'$(mol Kg^{-1})	0.2684
			$\sigma_{m_2'}$ (mol Kg^{-1})	0.0001
			$\Delta m_2 / \Delta m_1$	-5.4404
			$\sigma_{\Delta m_2 / \Delta m_1}$	0.1801

Table A15

m_1 (mmol Kg^{-1})	m_2 (mol Kg^{-1})	m_2' (mol Kg^{-1})	$\overline{m}_1$ (mmol Kg^{-1})	0.2634
0.2634	1.0533	1.0575	σ_{m_1} (mmol Kg^{-1})	0.0001
0.2634	1.0532	1.0569	$\overline{m}_2$ (mol Kg^{-1})	1.0533
0.2635	1.0537	1.0576	σ_{m_2} (mol Kg^{-1})	0.0003
0.2633	1.0529	1.0578	$\overline{m}_2'$ (mol Kg^{-1})	1.0575
			$\sigma_{m_2'}$ (mol Kg^{-1})	0.0004
			$\Delta m_2 / \Delta m_1$	−15.839
			$\sigma_{\Delta m_2 / \Delta m_1}$	1.8116

Table A16

m_1 (mmol Kg^{-1})	m_2 (mol Kg^{-1})	m_2' (mol Kg^{-1})	$\overline{m}_1$ (mmol Kg^{-1})	0.5432
0.5431	1.0756	1.0855	σ_{m_1} (mmol Kg^{-1})	0.0001
0.5431	1.0755	1.0842	$\overline{m}_2$ (mol Kg^{-1})	1.0850
0.5432	1.0758	1.0851	σ_{m_2} (mol Kg^{-1})	0.0006
0.5433	1.0760	1.0853	$\overline{m}_2'$ (mol Kg^{-1})	1.0757
			$\sigma_{m_2'}$ (mol Kg^{-1})	0.0002
			$\Delta m_2 / \Delta m_1$	−17.1872
			$\sigma_{\Delta m_2 / \Delta m_1}$	1.1453

Table A17

m_1 (mmol Kg^{-1})	m_2 (mol Kg^{-1})	m_2' (mol Kg^{-1})	$\overline{m}_1$ (mmol Kg^{-1})	0.7801
0.7798	1.0394	1.0510	σ_{m_1} (mmol Kg^{-1})	0.0004
0.7800	1.0396	1.0511	$\overline{m}_2$ (mol Kg^{-1})	1.0398
0.7807	1.0406	1.0523	σ_{m_2} (mol Kg^{-1})	0.0006
0.7801	1.0397	1.0522	$\overline{m}_2'$ (mol Kg^{-1})	1.0517
			$\sigma_{m_2'}$ (mol Kg^{-1})	0.0007
			$\Delta m_2 / \Delta m_1$	−15.1620
			$\sigma_{\Delta m_2 / \Delta m_1}$	1.1480

Table A18

m_1 (mmol Kg^{-1})	m_2(mol Kg^{-1})	m_2' (mol Kg^{-1})	$\overline{m}_1$(mmol Kg^{-1})	1. 1163
1. 1166	0. 9955	1. 0135	σ_{m_1} (mmol Kg^{-1})	0. 0003
1. 1164	0. 9953	1. 0143	$\overline{m}_2$(mol Kg^{-1})	0. 9952
1. 1164	0. 9953	1. 0140	σ_{m_2} (mol Kg^{-1})	0. 0003
1. 1158	0. 9948	1. 0139	$\overline{m}_2'$(mol Kg^{-1})	1. 0139
			$\sigma_{m_2'}$ (mol Kg^{-1})	0. 0003
			$\Delta m_2 / \Delta m_1$	−16. 7598
			$\sigma_{\Delta m_2 / \Delta m_1}$	0. 3878

Table A19

m_1 (mmol Kg^{-1})	m_2(mol Kg^{-1})	m_2' (mol Kg^{-1})	$\overline{m}_1$(mmol Kg^{-1})	2. 3566
2. 3536	0. 9357	0. 9760	σ_{m_1} (mmol Kg^{-1})	0. 0027
2. 3587	0. 9377	0. 9776	$\overline{m}_2$(mol Kg^{-1})	0. 9369
2. 3592	0. 9379	0. 9769	σ_{m_2} (mol Kg^{-1})	0. 0011
2. 3550	0. 9362	0. 9749	$\overline{m}_2'$(mol Kg^{-1})	0. 9763
			$\sigma_{m_2'}$ (mol Kg^{-1})	0. 0012
			$\Delta m_2 / \Delta m_1$	−16. 7460
			$\sigma_{\Delta m_2 / \Delta m_1}$	0. 6788

REFERENCES

References:

1. Munk, P., *Introduction to Macromolecular Science,* Wiley, New York **2001**
2. Tanford, C., *Physical Chemistry of Macromolecules,* Wiley, New York **1961**
3. Harris, J. M., *Poly(Ethylene Glycol) Chemistry: Biotechnical and Biomedical Applications,* Springer New York **1992**
4. Atkins, P.; de Paula, J., *Physical chemistry for the Life Sciences,* Oxford, New York **2006**
5. Tinoco, I. Jr.; Kenneth, S.; Wang, J. C., *Physical chemistry Principles and applications in biological Sciences,* Prentice Hall **1995**
6. Riès-Kautt, M.; Ducruix, A., *J. Biol. Chem.* **1989**, 264, 745
7. Herma, J. J., *Annu. Rev. Phys. Chem.* **1957**, 8, 179
8. Hey, M. J.; Jackson, D. P.; Yan, H., *Polymer* **2005,** 46, 2567
9. Kulkarni, A. M.; Chatterjee, A. P.; Schweizer, K. S.; Zukoski, C. F., *J. Chem. Phys.* **2000**, 113, 9863
10. Williams, C., *Ann. Rev. Phys. Chem.* **1981,** 32, 433
11. Thiyagarajan,P.; Chaiko, D. J.; Hjelm, R. P., *Macromolecules* **1995,** 28, 7730
12. Annunziata, O; Paduano, L; Albright, J.G., *J. Phys. Chem. B*, **2006** 110, 16139
13. Annunziata, O; Paduano, L.; Pearlstein, A. J.; Miller,D.G.; Albright, J.G., *J. Phys. Chem. B* **2006,** *110,* 1405-1415
14. Fischer, V.; Borchard, W., *J. Phys. Chem. B* **2000**, 104, 4463
15. Hakem, I. F.; Lal, J.; Bockstaller, M. R., *Macromolecules* **2004**, 37, 8431

16. Shimizu, S., *J. Chem. Phys.* **2004**, 121, 9147

17. Albright, J. G.; Annunziata, O.; Miller, D. G.; Paduano, L.; Pearlstein A. J., *J. Am. Chem. Soc.* **1999**, 121, 3256.

18. Annunziata, O.; Paduano, L.; Pearlstein, A. J.; Miller, D. G.; Albright, J. G., *J. Am. Chem. Soc*. **2000**, 122, 5916.

19. Paduano, L.; Annunziata, O.; Pearlstein, A. J.; Miller, D. G.; Albright, J. G., *J. Crystal Growth* **2001**, 232, 273.

20. Annunziata, O.; Asherie, N.; Lomakin, A.; Pande, J.; Ogun O.; Benedek, G. B., *Proc. Natl. Acad. Sci.* USA **2002**, 99, 14165-14170.

21. Annunziata, O.; Albright, J. G., *Ann. N. Y. Acad. Sci.* **2002**, *974*, 610

22. Roe, S., *Protein Purification Techniques* **2001**. Oxford, Oxford.

23. Riès-Kautt, M.; Ducruix, A., *J. Biol. Chem*. **1989**, 264, 745

24. Warren, P. B., *J. Phys.: Condens. Matter* **2002**, 14, 7617

25. Vaney, M. C.; Broutin, I.; Retailleau, P.; Douangamath, A.; Lafont, S.; Hamiaux, C.; Prange, T.; Ducruix, A.; Riès-Kautt, M., *Acta Cryst.* **2001**, D57, 929

26. Riès-Kautt, M.; Ducruix, A., *J. Crys. Growth* **1991**, 110, 20

27. Vekilov, P.G.; Monaco, L.A.; Thomas, B.R.; Stojanoff, V.; Rosenberger, F., *Acta Cryst.* **1996**, D52, 785

28. Uchegbu, I. F.; Schätzlein, A. G., *Polymers in Drug Delivery* **2006**, CRC Press

29. Annunziata,O.; Paduano, L.; Albright, J. G., *J. Phys. Chem. B* **2007**, 111, 10591

30. Parsegian, V. A.; Rand, R. P.; Rau. D. C., *Proc. Natl. Acad. Sci. USA* **2000**, 97, 3987

31. Timasheff, S. N., *Proc. Natl. Acad. Sci. USA*, **2002**, 99, 9721

32. Schellman, J. A., *Biophys. J*., **2003,** 85, 108

33. Record, M. T. Jr.; Anderson, C. F., *Biophys. J.* **1995** 68, 786–794.

34. Arakawa, T.; Bhat, R.; Timasheff, S. N., *Biochemistry* **1990**, 29, 1914

35. Arakawa, T.; Timasheff; S. N., *Biochemistry* **1984**, 23, 5912.

36. Arakawat, T.; Timasheff, S. N., *Biochemistry* **1985,** *24,* 6756-6762

37. Courtenay, E. S.; Capp, M. W.; Anderson, C. F.; Record, M. T., Jr., *Biochemistry* **2000** 39, 4455–4471

38. Record, M. T., Jr., *Adv. Protein Chem.* **1998** 51, 281–353.

39. Courtenay, E. S.; Capp, M. W.; Saecker, R. M.; Record, T. M., Jr., *Proteins Struct. Funct. Genet.* **2000** 41, 72–85.

40. Tyrell, H. J. V.; Harris, K.R., *Diffusion in Liquids* **1984** Butterworths, London

41. Miller, D. G.; Albright, J. G., *In Measurement of the Transport Properties of Fluids*: *Experimental Thermodynamics*; Wakeham, W. A., Nagashima, A., Sengers, J. V., Eds. Blackwell Scientific Publications, Oxford, **1991**, 272-294.

42. Squires, T.M.; Quake, S.R., *Reviews of Modern Physics*, **2005,** 77, 977

43. Hansen, C.; Quake, S. R., Curr. *Opin. Struct. Biol*, **2003,** 13, 538

44. Jiang, Y.; Woronicz, J.D.; Liu, W.; Goeddel, D.V., *Science*, **1999**, 283, 544

45. Atencia, J.; Beebe, D. J., *Nature*, **2005**, 437, 29

46. Whitesides, G. M., *Nature*, **2006**,442, 27

47. Israelachvili, J., *Proc. Natl. Acad. Sci. USA* **1997,** 94, 8378–8379,

48. Vergara,A.; Annunziata, O.; Paduano, L.; Miller, D. G.; Albright, J. G.; Sartorio, R., *J. Phys. Chem. B*, **2004**, 108, 2764

49. Annunziata, O., *Ph.D. dissertation* **2001**, Texas Christian Univ.

50. Forsythe, E. L.; Judge, R. A.; Pusey, M. L., *J. Chem. Eng. Data* **1999**, *44*, 637

51. Miller, D. G., *J. Phys. Chem.* **1966**, *70*, 2639

52. Palmer, K. J.; Ballantyne, M.; Galvin, J. A., *J. Am. Chem. Soc.* **1948**, *70*, 906.

53. Flory, P. J., *J. Am. Chem. Soc.* **1940**,62,1561

54. Vergara, A.; Paduano, L.; Sartorio, R.; Vitagliano, V., *J. Phys. Chem. B* **1999**,103, 8732

55. Kawaguchi S.; Imai G.; Suzuki J.; Miyahara A.; Kitano T.; Ito K., *Polymer* **1997** 38, 2885

56. Tanaka, S.; Ataka ,M.; Onuma, K.; Kubota, T., *Biophysical Journal* **2003,** 84, 3299

57. Annunziata,O.; Buzatu, D.; Albright, J. G., *Langmuir*, **2005**, 21, 12085

58. Onsager, L., *Phys. Rev.* **1931**, 38, 2265

59. de Groot, S. R.; Mazur, P., *Non-equilibrium Thermodynamics* North-Holland, Amsterdam, **1962**

60. Wendt, R.P.; Gosting, L.J., *J. Physical Chemistry* **1959**, 63, 1959

61. Fujita, H.; Gosting, L.J., *J. Phys. Chem.* **1960**, 64, 1256

62. Kirkwood, J. G.; Baldwin, R. L.; Dunlop, P. J.; Gosting, L. J.; Kegeles, G., *J. Chem. Phys.* **1960**, *33*, 1505

63. Miller, D. G.; Vitagliano, V.; Sartorio, R., *J. Phys. Chem.* **1986**, *90*, 1509

64. Fujita, H.; Gosting L. J., *J. Am. Chem. Soc.* **1956**, *78*, 1099

65. Leaist, D. G., *J. Colloid and Interface Science* **1986**, 111, 240

66. Miller, D. *G*., *J. Phys. Chem.* **1959**, 63, 570

67. Woolf, L. A.; Miller, D. G.; Gosting, L. J., *J. Am. Chem. Soc.* **1962**, *84*, 317.

68. Nernst, W. Z., *Phys. Chem.* **1889**, 4, 129

69. Hartley, G. S.; Crank, J., *Trans. Faraday Soc.* **1949**, 45, 801

70. Robinson, R. A.; Stokes, R. H., *Electrolyte Solutions* Academic Press, New York, **1955**

71. Gosting, L., *J. Adv. Protein Chem.* **1956**, 11, 429

72. Dunlop, P. J.; Gosting, L. J., *J. Phys. Chem.* **1959**, *63*, 86

73. Rard, J. A.; Miller, D. G., *J. Chem. Eng. Data* **1980**, 25, 211

74. Gosting, L. J.; Kim, H.; Loewenstein, M. A.; Reinfelds, G.; Revzin, A., *Rev. Sci. Instru.* **1973**, *44*, 1602

75. Baldwin, R.L.; Dunlop, P.J.; Gosting, L.J., *J. Am. Chem. Soc.* **1955**, 77, 5238

76. Miller, D. G.; Albright, J. G.; Mathew, R.; Lee, C. M.; Rard, J. A.; Eppstein, L. B., *J. Phys. Chem.* **1993**, *97*, 3885.

77. Rard, J. A.; Miller, D.G., *Journal of Solution Chemistry* **1979**, 8, 10

78. Creeth, J.M., *J. Am. Chem. Soc.* **1955**, 77, 6428

79. Lin,D.Q.; Zhu,Z.Q.; Mei, L.H.; Yang L.R., *J. Chem. Eng. Data*. **1996** 41 1040

80. Rard, J. A., *J. Chem. Eng. Data* **2003,** 48, 158

81. Palmer，D. A.; Archer, D. G.; Rard, J. A., *J. Chem. Eng. Data* **2002,** 47, 1425

82. Rard, J. A.; Miller, D.G., *J. Chem. Eng. Data* **2005,** *50*, 1162-1170

83. Seidel, J.; Rossner, K.; Kuschel, F., *J. Chem. Eng. Data*. **1985**, 30, 209-292

84. Zhang, H.L.; Han, S.J., *J. Chem. Eng. Data* **1996**, *41*, 516

85. Tanford, C.; Wagner, M. L., *J. Am. Chem. Soc*. **1954**, *76*, 3331.

VITA

VITA

Cong Tan was born on March 11, 1982 in Xiangfan, Hubei, China. She is the daughter of Yong Tan and Junhua Yu. A 2000 graduate of Xiangfan No. 4 High School， Hubei，China, she entered the University of Science and Technology of China (USTC), Hefei China, majoring in Physical Chemistry. She graduate from USTC and received a bachelor degree in 2004.

In the August 2000, she enrolled in the graduate study at Texas Christian University and joined the Dr. Annunziata's group. While working under the guidance of Dr. Annunziata, she held a teaching assistantship in 2005-2006.

ABSTRACT

ABSTRACT

THE EFFECT OF SALT ON THE CHEMICAL POTENTIAL OF NEUTRAL MACROMOLECULES DETERMINED BY TERNARY DIFFUSION COEFFICIENTS

By Cong Tan, M.S., 2007
Department of Chemistry, Texas Christian University

Thesis Advisor: Onofrio Annunziata, Assistant Professor of Chemistry

Diffusion of macromolecules in aqueous solutions is important for many laboratory, biological, and manufacturing applications. However, aqueous solutions containing macromolecules often contain other additives. An important feature of these multicomponent mixtures is the macromolecule-additive interaction. Due to this interaction, the additive concentration gradient can induce macromolecule diffusion and vice versa. This phenomenon is known as coupled diffusion and is described by multicomponent diffusion coefficients. This thesis reports the experimental investigation of multicomponent diffusion coefficients for the Poly(ethylene glycol)-KCl-water ternary system at 25 ºC using Rayleigh interferometry. These coefficients were used to determine PEG-salt interaction. Furthermore, isopiestic experiments were performed to demonstrate that multicomponent diffusion yields accurate thermodynamic parameters. Fundamentally, this work has provided a significant contribution to the connection between diffusion and thermodynamics. Moreover, significant coupled diffusion between PEG and KCl was observed due to a large PEG hydration. Thus, PEG concentration gradients can be used to induce diffusion of other molecules in water for potential applications in controlled-release and micro-fluidic technologies.